

Convolutional Neural Associative Memories: Massive Capacity with Noise Tolerance

Amin Karbasi

E-mail: amin.karbasi@ethz.ch

Computer Science Department

Swiss Federal Institute of Technology Zurich, 8092 Zurich, Switzerland

Amir Hesam Salavati

E-mail: hesam.salavati@epfl.ch

Computer and Communication Sciences Department

Ecole Polytechnique Federale de Lausanne, Lausanne, 1015, Switzerland

Amin Shokrollahi

E-mail: amin.shokrollahi@epfl.ch

Computer and Communication Sciences Department

Ecole Polytechnique Federale de Lausanne, Lausanne, 1015, Switzerland

April 4, 2024

Abstract

The task of a neural associative memory is to retrieve a set of previously memorized patterns from their noisy versions using a network of neurons. An ideal network should have the ability to 1) learn a set of patterns as they arrive, 2) retrieve the correct patterns from noisy queries, and 3) maximize the pattern retrieval capacity while maintaining the reliability in responding to queries. The majority of work on neural associative memories has focused on designing networks capable of memorizing any set of randomly chosen patterns at the expense of limiting the retrieval capacity.

In this paper, we show that if we target memorizing only those patterns that have inherent redundancy (i.e., belong to a subspace), we can obtain all the aforementioned properties. This is in sharp contrast with the previous work that could only improve one or two aspects at the expense of the third. More specifically, we propose framework based on a convolutional neural

network along with an iterative algorithm that learns the redundancy among the patterns. The resulting network has a retrieval capacity that is *exponential* in the size of the network. Moreover, the asymptotic error correction performance of our network is *linear* in the size of the patterns. We then extend our approach to deal with patterns lie *approximately* in a subspace. This extension allows us to memorize datasets containing natural patterns (e.g., images). Finally, we report experimental results on both synthetic and real datasets to support our claims.

1 Introduction

The ability of neuronal networks to memorize a large set of patterns and reliably retrieve them in the presence of noise, has attracted a large body of research over the past three decades to design artificial neural associative memories with similar capabilities. Ideally, a perfect neural associative memory should be able to *learn* patterns, have a large pattern retrieval *capacity* and be *noise-tolerant*. This problem, called "associative memory", is in spirit very similar to reliable information transmission faced in communication systems where the goal is to efficiently decode a set of transmitted patterns over a noisy channel.

Despite this similarity and common methods deployed in both fields (e.g., graphical models, iterative algorithms, to name a few), we have witnessed a huge gap between the efficiency achieved by them. More specifically, by deploying modern coding techniques, it was shown that the number of reliably transmitted patterns over a noisy channel can be made *exponential* in n , the length of the patterns. This was particularly achieved by imposing redundancy among transmitted patterns. In contrast, the maximum number of patterns that can be reliably memorized by most current neural networks scales *linearly* in the size of the patterns. This is due to the common assumption that a neural network should be able to memorize *any* subset of patterns drawn randomly from the set of all possible vectors of length n (see, for example Hopfield, 1982, Venkatesh and Psaltis, 1989, Jankowski et al., 1996, Muezzinoglu et al., 2003).

Recently, Kumar et al. (2011) suggested a new formulation of the problem where only a suitable set of patterns was considered for storing. To enforce the set of constraints, they formed a bipartite graph (as opposed to a complete graph considered in the earlier work) where one layer feeds the patterns to the network and the other takes into account the inherent structure. The role of bipartite graph is indeed similar to the Tanner graphs used in modern coding techniques (Tanner, 1981). Using this model, Kumar et al. (2011) provided evidence that the resulting network can memorize an exponential number of patterns at the expense of correcting only a *single* error during the recall phase. By introducing a multi-layer

structure, Salavati and Karbasi (2012) could further improve the error correction performance to *constant* number of errors.

In this paper, similar to the model considered by Kumar et al. (2011), we only consider a set of patterns with weak minor components, i.e., patterns that lie in a subspace. By making use of this inherent redundancy

- We introduce the first convolutional neural associative network with provably exponential storage capacity.
- We prove that our architecture can correct a linear fraction of errors.
- We develop an *online* learning algorithm with the ability to learn patterns as they arrive. This property is specifically useful when the size of the dataset is massive and patterns can only be learned in a streaming manner.
- We extend our results to the case where patterns lie *approximately* in a subspace. This extension in particular allows us to efficiently memorize datasets containing natural patterns.
- We evaluate the performance of our proposed architecture and the learning algorithm through numerical simulations.

We provide rigorous analysis to support our claims. The storage capacity and error correction performance of our method is information-theoretically order optimum, i.e., no other method can significantly improve the results (except for constants). Our learning algorithm is an extension of the subspace learning method proposed by Oja and Kohonen (1988), with an additional property of imposing the learned vectors to be *sparse*. The sparsity is essential during the noise-elimination phase.

The remainder of this paper is organized as follows. In Section 2 we provide an overview of the related work in this area. In Section 3 we introduce our notation and formally state the problems that is the focus of this work, namely, learning phase, recall phase, and storage capacity. We present our learning algorithm in Section 4 and our error correction method in Section 5. Section 6 is devoted to the pattern retrieval capacity. We then report our experimental results on synthetic and natural datasets in Section 7. Finally, all the proofs are provided in Section 8.

2 Related Work

The famous Hopfield network was among the first auto-associative neural mechanisms capable of learning a set of patterns and recalling them subsequently (Hopfield, 1982). By employing the Hebbian learning rule (Hebb, 1949), Hopfield

considered a neural network of size n with binary state neurons. It was shown by McEliece et al. (1987) that the capacity of a Hopfield network is bounded by $C = (n/2 \log(n))$. Due to the low capacity of Hopfield networks, extension of associative memories to non-binary neural models has also been explored, with the hope of increasing the pattern retrieval capacity. In particular, Jankowski et al. (1996) investigated a complex-valued neural associative memory where each neuron can be assigned a multivalued state from the set of complex numbers. It was shown by Muezzinoglu et al. (2003) that the capacity of such networks can be increased to $C = n$ at the cost of a prohibitive weight computation mechanism. To overcome this drawback, a Modified Gradient Descent learning Rule (MGDR) was devised by Lee (2006).

Recently, in order to increase the capacity and robustness, a line of work considered exploiting the inherent structure of the patterns. This is done by either making use of the correlations among the patterns or memorizing only those patterns that have some sort of redundancy. Note that they differ from the previous work in one important aspect: not any possible set of patterns is considered for learning, but only those with common structures. By employing neural cliques, Gripon and Berrou (2011) were among the first to demonstrate that considerable improvements in the pattern retrieval capacity of Hopfield networks is possible, albeit still not passing the polynomial boundary on the capacity, i.e., $C = O(n^2)$.

Similar idea was proposed by Venkatesh (1994) for learning semi-random patterns. This boost to the capacity is achieved by dividing the neural network into smaller fully interconnected *disjoint* blocks. Using this idea, the capacity is increased to $\Theta(b^{n/b})$, where $b = \omega(\ln n)$ is the size of clusters. Nonetheless, it was observed that this improvement comes at the price of limited noise tolerance capabilities.

By deploying higher order neural models, in contrast to the pairwise correlation considered in Hopfield networks, Peretto and Niez (1986) showed that the storage capacity can be improved to $C = O(n^{p-2})$, where p is the degree of correlation. In such models, the state of the neurons not only depends on the state of their neighbors, but also on the correlations among them. However, the main drawback of this work lies in the prohibitive computational complexity of the learning phase. Recently, Kumar et al. (2011) introduced a new model based on bipartite graphs to capture higher order (linear) correlations without the prohibitive computational complexity in the learning phase. The proposed model was further improved later (Kumar et al., 2014). Under the assumption that the bipartite graph is fully known, sparse, and expander, the proposed algorithm by Kumar et al. (2011) increased the pattern retrieval capacity to $C = O(a^n)$, for some $a > 1$. In addition to those restrictive assumptions, the performance of the recall phase was still below par.

In this paper, we introduce a convolutional neural network, capable of memorizing an exponential number of structured patterns while being able to correct a linear fraction of noisy neurons. Similar to the model considered by Kumar et al. (2011), we assume that patterns lie in a low dimensional subspace. Note that a network of size n , where each neuron can hold a finite number of states, is capable of memorizing at most an exponential number of patterns in n . Also, correcting a linear fraction of noisy nodes of the network is the best we can hope for. In addition, and more importantly in practice, we extend our results to the set of patterns that only approximately belong to a subspace.

It is worth mentioning that learning a set of input patterns with robustness against noise is not just the focus of neural associative memories. For instance, Vincent et al. (2008) proposed an interesting approach to extract robust features in autoencoders. Their approach is based on *artificially introducing* noise during the learning phase and let the network learn the mapping between the corrupted input and the correct version. This way, they shifted the burden from the recall phase to the learning phase. We, in contrast, consider another form of redundancy and enforce a suitable pattern structure that helps us design faster algorithms and derive necessary conditions that help us *guarantee* to correct a linear fraction of noise without previously being exposed to.

Although our neural architecture is not technically considered a Deep Belief Network (DBN), it shares some similarities. DBNs are typically used to extract/classify features by the means of several consecutive stages (e.g., pooling, rectification, etc). Having multiple stages help the network to learn more interesting and complex features. An important class of DBNs are convolutional DBNs. The input layer (also known as the receptive field) is divided into multiple overlapping patches and the network extracts features from each patch (Jarrett et al., 2009). Since we divide the input patterns into a few overlapping smaller clusters, our model is similar to those of convolutional DBNs. Furthermore, we also learn multiple *features* (in our case dual vectors) from each patch where the feature extractions differ over different patches. This is indeed very similar to the approach proposed by Le et al. (2010). In contrast to convolutional DBNs, the focus of this work is not classification but rather recognition of the *exact* patterns from their noisy versions. Moreover, in most DBNs, we not only have to find the proper dictionary for classification, but we also need to calculate the features for each input pattern. This alone increases the complexity of the whole system, especially if denoising is part of the objective. In our model, however, the dictionary is defined in terms of dual vectors. Consequently, previously memorized patterns are computationally easy to recognize as they yield the all-zero vector in the output of the feature extraction stage. In other words, a non-zero output can only happen if the input pattern is noisy. Another advantage of our model over DBNs is a much faster

learning phase. More precisely, by using a single layer with overlapping clusters in our model the information diffuses gradually in the network. The same criteria is achieved in DBNs by constructing several stages (Socher et al., 2011).

3 Problem Formulation

In this section, we set our notation and formally define the learning phase, recall phase, and the storage capacity.

3.1 Learning Phase

Throughout this paper, each pattern is denoted by an integer-valued vector $x = (x_1, x_2, \dots, x_n)$ of length n where $x_i \in \mathcal{Q} = \{0, \dots, Q - 1\}$ for $i = 1, \dots, n$ and Q is a non-negative integer. In words, the set \mathcal{Q} could be thought of as the short term firing rate of neurons. Let $\{s_i\}_i^n$ denote the states of neurons in a neural network G . Each neuron updates its state based on the states of its neighbors. More precisely, a neuron j first computes a weighted sum $\sum_{i \in \mathcal{N}(j)} w_{j,i} s_i$ and then applies a nonlinear *activation* function $f : \mathbb{R} \rightarrow \mathcal{Q}$, i.e.,

$$s_j = f \left(\sum_{i \in \mathcal{N}(j)} w_{j,i} s_i \right).$$

Here, $w_{j,i}$ is the weight of the neural connection between neurons j and i , and $\mathcal{N}(j)$ denotes the neighbors of neuron j in G . There are several possible activation functions used in the literature including, but not limited to, linear, threshold, logistic, and tangent hyperbolic functions.

We denote the dataset of the patterns by the $C \times n$ dimensional matrix \mathcal{X} , where patterns are stored as the rows. Our goal in this work is to memorize patterns with strong *local correlation* among the entries. More specifically, we divide the entries of each pattern x into L *overlapping sub-patterns* of lengths n_1, \dots, n_L , so that $\sum n_i \geq n$. Note that due to overlaps, an entry in a pattern can be a member of multiple sub-patterns, as shown in Figure 1. We denote the i -th sub-pattern by

$$x^{(i)} = (x_1^{(i)}, x_2^{(i)}, \dots, x_{n_i}^{(i)}).$$

To enforce local correlations, we assume that the sub-patterns $x^{(i)}$ form a subspace of dimension $k_i < n_i$. This is done by imposing linear constraints on each cluster.

These linear constraints are captured during the learning phase in the form of dual vectors. More specifically, we find a set of non-zero *vectors* $w_1^{(i)}, w_2^{(i)}, \dots, w_{m_i}^{(i)}$

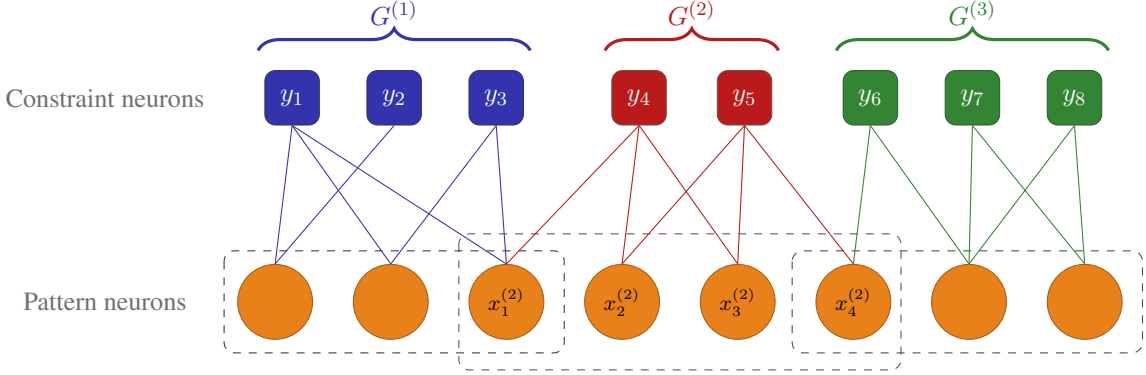


Figure 1: Bipartite graph G . In this figure we see three subpatterns $x^{(1)}, x^{(2)}, x^{(3)}$ along with corresponding clusters $G^{(1)}, G^{(2)}, G^{(3)}$. The subpattern $x^{(2)}$ has overlaps with both $G^{(1)}$ and $G^{(3)}$. The weights $w_{i,j}$ are chosen to ensure that $W \cdot x = 0$ for all patterns x lying in a subspace.

that are orthogonal to the set of sub-patterns $x^{(i)}$, i.e.,

$$y_j^{(i)} = \langle w_j^{(i)}, x^{(i)} \rangle = 0, \quad \forall j \in [m_i] \forall i \in [L], \quad (1)$$

where $[q]$ denotes the set $\{1, 2, \dots, q\}$ and $\langle \cdot, \cdot \rangle$ represents the inner product.

The weight matrix $W^{(i)}$ is constructed by placing all dual vectors next to each other, i.e.,

$$W^{(i)} = [w_1^{(i)} | w_2^{(i)} | \dots | w_{m_i}^{(i)}]^\top.$$

Equation (1) can be written equivalently as

$$W^{(i)} \cdot x^{(i)} = 0.$$

Cluster i represents the bipartite graph $G^{(i)}$ with the connectivity matrix $W^{(i)}$. In the next section, we develop an iterative algorithm to learn the weight matrices $W^{(1)}, \dots, W^{(L)}$, while encouraging sparsity within each connectivity matrix $W^{(i)}$.

One can easily map the local constraints imposed by the $W^{(i)}$'s into a global constraint by introducing a global weight matrix W of size $m \times n$. The first m_1 rows of the matrix W correspond to the constraints in the first cluster, rows $m_1 + 1$ to $m_1 + m_2$ correspond to the constraints in the second cluster, and so forth. Hence, by inserting zero entries at proper positions, we can construct the global constraint matrix W . We will use both the local and global connectivity matrices to eliminate noise in the recall phase.

3.2 Recall Phase

In the recall phase a noisy version, say \hat{x} , of an already learned pattern $x \in \mathcal{X}$ is given. Here, we assume that the noise is an additive vector of size n , denoted by e , whose entries assume values independently from $\{-1, 0, +1\}$ ¹ with corresponding probabilities $p_{-1} = p_{+1} = p_e/2$ and $p_0 = 1 - p_e$. In other words, each entry of the noise vector is set to ± 1 with probability p_e . The ± 1 values are chosen to simplify the analysis. Our approach can be easily extended to other integer-valued noise models.

We denote by $e^{(i)}$, the realization of noise on the sub-pattern $x^{(i)}$. In formula, $\hat{x} = x + e$.² Note that $W \cdot \hat{x} = W \cdot e$ and $W^{(i)} \cdot \hat{x}^{(i)} = W^{(i)} \cdot e^{(i)}$. Therefore, the goal in the recall phase is to remove the noise e and recover the desired pattern x . This task will be accomplished by exploiting the facts that a) we have chosen the set of patterns \mathcal{X} to satisfy the set of constraints $W^{(i)} \cdot x^{(i)} = 0$ and b) we opted for sparse neural graphs $G^{(i)}$ during the learning phase. Based on these two properties, we develop the first recall algorithm that corrects a linear fraction of noisy entries.

3.3 Capacity

The last issue we look at in this work is the retrieval capacity C of our proposed method. Retrieval or critical storage capacity is defined as the maximum number of patterns that a neural network is able to store without having (significant) errors in returned answers during the recall phase. Hence, the storage capacity $C(n)$ is usually measured in terms of the network size n . It is well known that the retrieval capacity is affected by certain considerations about the neural network, including the range of values or states for the patterns, inherent structure of patterns, and topology of neural networks. In this work, we show that a careful combination of patterns' structure and neural network topology leads to an exponential storage capacity in the size of the network.

4 The Learning Algorithm

In this section, we develop an algorithm for learning the weight matrix $W^{(\ell)}$ of a given cluster ℓ . By our assumptions, the sub-patterns lie in a subspace of dimension $k_\ell \leq n_\ell$. Hence we can adopt the iterative algorithm proposed by Oja

¹In our experiments, we have considered larger integer values for noise as well, i.e., $\{-q, \dots, 0, \dots, q\}$, for some $q \in \mathbb{N}$. The ± 1 noise model here is considered to simplify the notations and analysis.

²Note that since entries of \hat{x} should be between 0 and $Q - 1$, we cap values below 0 and above $Q - 1$ to 0 and $Q - 1$, respectively.

and Karhunen (1985) and Xu et al. (1991) to learn the corresponding null space. However, in order to ensure the success of the denoising algorithm proposed in Section 5, we require $W^{(l)}$ to be sparse. To this end, the objective function shown below has a penalty term to encourage sparsity. Furthermore, we are not seeking an orthogonal *basis* as in the approach proposed by Xu et al. (1991). Instead, we wish to find m_ℓ vectors $w^{(\ell)}$ that are orthogonal to the (sub-) patterns. Hence, the optimization problem for finding a constraint *vector* $w^{(\ell)}$ can be formulated as follows:

$$\min_{w^{(\ell)}} \sum_{x \in \mathcal{X}} |\langle x^{(\ell)}, w^{(\ell)} \rangle|^2 + \eta g(w^{(\ell)}), \quad (2)$$

$$\text{s.t.} \quad \|w^{(\ell)}\|_2 = 1. \quad (3)$$

In the above problem, $x^{(\ell)}$ is a sub-pattern of x drawn from the training set \mathcal{X} , $\langle \cdot, \cdot \rangle$ indicates the inner product, η is a positive constant, and $g(\cdot)$ is the penalty term to favor sparse results. In this paper, we consider

$$g(w^{(\ell)}) = \sum_{i=1}^n \tanh(\sigma(w_i^{(\ell)})^2).$$

It is easy to see that for large σ , the function $\tanh(\sigma(w_i^{(\ell)})^2)$ approximates $|\text{sign}(w_i^{(\ell)})|$ (as shown in Figure 2). Therefore, the larger σ gets, the closer $g(w^{(\ell)})$ will be to $\|\cdot\|_0$. Another popular choice, widely used in compressed sensing (see, for example, Donoho, 2006 and Candès and Tao, 2006), is to pick $g(w^{(\ell)}) = \|w^{(\ell)}\|_1$. Note that the optimization problem (2) without the constraint (3) has the trivial solution $w^{(\ell)} = \mathbf{0}$ where $\mathbf{0}$ is the all-zero vector.

To minimize the objective function shown in (2) subject to the norm constraint (3) we use stochastic gradient descent and follow a similar approach to that of Xu et al. (1991). By calculating the derivative of the objective function and considering the updates required for each randomly picked pattern x , we will obtain the following iterative algorithm:

$$y^{(\ell)}(t) = \langle x^{(\ell)}(t), w^{(\ell)}(t) \rangle, \quad (4)$$

$$\tilde{w}^{(\ell)}(t+1) = w^{(\ell)}(t) - \alpha_t \left(2y^{(\ell)}(t)x^{(\ell)}(t) + \eta \Gamma(w^{(\ell)}(t)) \right), \quad (5)$$

$$w^{(\ell)}(t+1) = \frac{\tilde{w}^{(\ell)}(t+1)}{\|\tilde{w}^{(\ell)}(t+1)\|_2}. \quad (6)$$

In the above equations, t is the iteration number, $x^{(\ell)}(t)$ is the subpattern of a pattern $x(t)$ drawn at iteration t , α_t is a small positive constant, and $\Gamma(w^{(\ell)}) =$

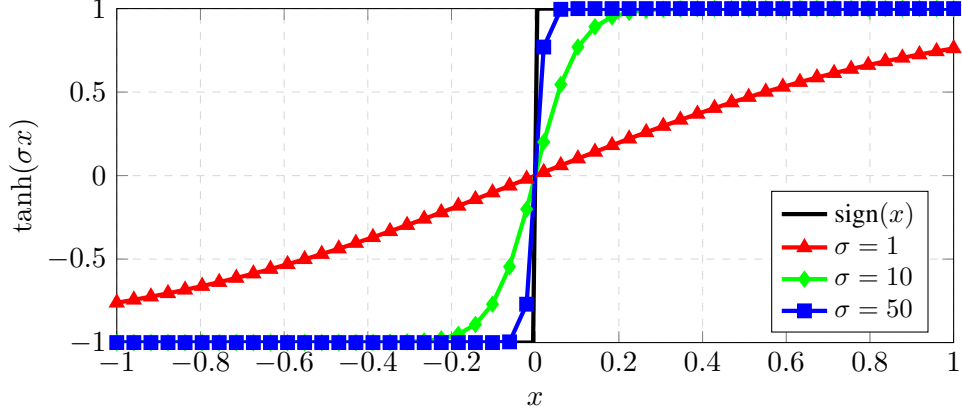


Figure 2: Approximation of $\text{sign}(x)$ by $\tanh(\sigma x)$. As we increase the value of σ the approximation becomes more accurate.

$\nabla g(w^{(\ell)})$ is the gradient of the penalty term. The function $\Gamma(w^{(\ell)})$ encourages sparsity. To see why, consider the i -th entry of $\Gamma(\cdot)$, namely,

$$\begin{aligned}\Gamma_i(z_i) &= \frac{\partial g(z)}{\partial z_i} \\ &= 2\sigma z_i(1 - \tanh^2(\sigma z_i^2)).\end{aligned}$$

Note that $\Gamma_i \simeq 2\sigma z_i$ for relatively small values of z_i , and $\Gamma_i \simeq 0$ for larger values of z_i (see Figure 3).

Thus, for proper choices of η and σ , equation (5) suppresses small entries of $w^{(\ell)}(t)$ towards zero and favors sparser results. To further simplify the iterative equations (4), (5), (6) we approximate the function $\Gamma(w^{(\ell)}(t))$ with the following threshold function (shown in Figure 4):

$$\Gamma_i(z_i, \theta_t) = \begin{cases} z_i & \text{if } |z_i| \leq \theta_t; \\ 0 & \text{otherwise.} \end{cases}$$

where θ_t is a small positive threshold. Following the same approach taken by Oja and Karhunen (1985) we assume that α_t is small enough so that equation (6) can be expanded as powers of α_t . Also note that the inner product $\langle w^{(\ell)}(t), \Gamma(w^{(\ell)}(t), \theta_t) \rangle$ is small so in the power expansion we can omit the term $\alpha_t \eta \left(\langle w^{(\ell)}(t), \Gamma(w^{(\ell)}(t), \theta_t) \rangle \right) w^{(\ell)}(t)$.

By applying the above approximations we obtain an iterative learning algorithm shown in Algorithm 1. In words, $y^{(\ell)}(t)$ is the projection of $x^{(\ell)}(t)$ onto

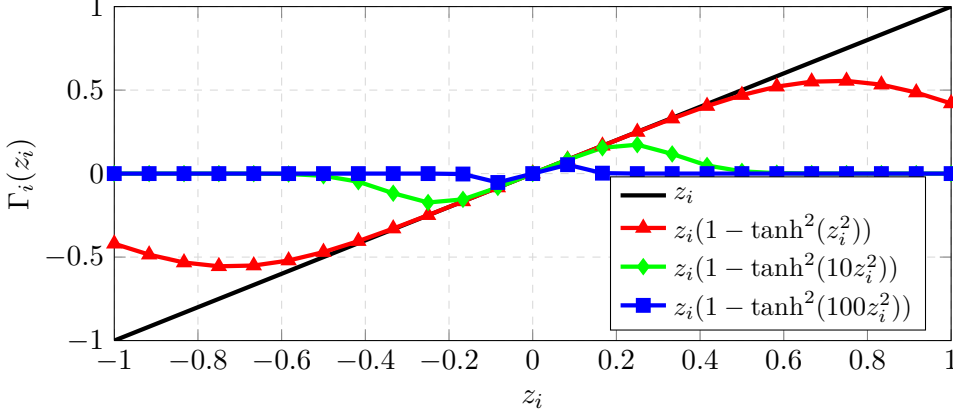


Figure 3: The sparsity penalty $\Gamma_i(z_i)$ suppresses small values of z_i towards zero. Note that as σ gets larger, the support of $\Gamma_i(z_i)$ gets smaller.

$w^{(\ell)}(t)$. If for a given data vector $x^{(\ell)}(t)$ the projection $y^{(\ell)}(t)$ is non-zero, then the weight vector will be updated in order to reduce this projection.

4.1 Convergence Analysis

Our main idea for proving the convergence of the learning algorithm is to consider the *learning cost function* defined as follows:

$$E(t) = E(w^{(\ell)}(t)) = \frac{1}{C} \sum_{\mu=1}^C \left(\langle w^{(\ell)}(t), x^\mu \rangle \right)^2$$

We show that as we gradually learn patterns from the data set \mathcal{X} , the cost function $E(t)$ goes to zero. In order to establish this result we need to specify the learning rate α_t . In what follows, we assume that $\alpha_t = \Omega(1/t)$ so that $\sum_t \alpha_t \rightarrow \infty$ and $\sum_t \alpha_t^2 < \infty$. We first show that the weight vector $w^{(\ell)}(t)$ never becomes zero, i.e., $\|w^{(\ell)}(t)\|_2 > 0$ for all t .

Lemma 1 Assume that $\|w^{(\ell)}(0)\|_2 > 0$ and $\alpha_0 < 1/\eta$. Then for all iterations t , we have $\alpha_t < \alpha_0 < 1/\eta$ and $\|w^{(\ell)}(t)\|_2 > 0$.

As mentioned earlier, all the proofs are given in Section 8.

The above lemma ensures that if we reach $E(t) = 0$ for some iteration t , it is not the case that $w^{(\ell)}(t) = \underline{0}$. Next, we prove the convergence of Algorithm 1 to a minimum $\hat{w}^{(\ell)}$ for which $E(\hat{w}^{(\ell)}) = 0$.

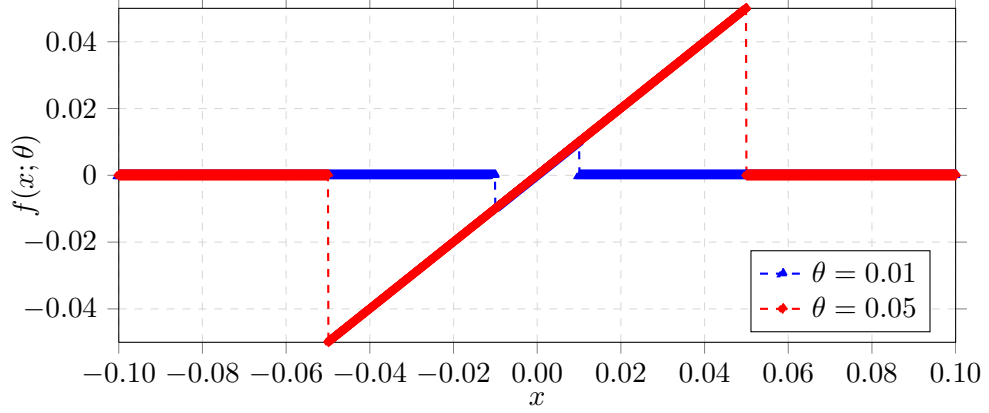


Figure 4: The soft threshold function $f(x, \theta)$ for two different values of θ .

Theorem 2 *Under the conditions of Lemma 2, the learning Algorithm 1 converges to a local minimum $\hat{w}^{(\ell)}$ for which $E(\hat{w}^{(\ell)}) = 0$. Moreover $\hat{w}^{(\ell)}$ is orthogonal to all the patterns in the data set \mathcal{X} .*

We should note here that a similar convergence result can be proven without introducing the penalty term $g(w^{(\ell)})$. However, our recall algorithm crucially depends on the sparsity level of learned $w^{(\ell)}$'s. As a consequence we encouraged sparsity by adding the penalty term $g(w^{(\ell)})$. Our experimental results in Section 7 show that in fact this strategy works perfectly and the learning algorithm results in sparse solutions.

In order to find m_ℓ constraints required by the learning phase, we need to run Algorithm 1 *at least* L times. In practice, we can perform this process in parallel, to speed up the learning phase. It is also more meaningful from a biological point of view, as each constraint neuron can act independently from the others. Although running Algorithm 1 in parallel may result in redundant constraints, our experimental results show that by starting from different random initial points, the algorithm converges to linearly independent constraints almost surely.

5 Recall Phase

Once the learning phase is finished, the weights of the neural graphs are fixed. Thus, during the recall phase we assume that the connectivity matrix for each cluster i (denoted by $W^{(i)}$) has been learned and satisfies (1).

The recall phase of our proposed model consists of two parts: intra-cluster and inter-cluster. During the intra-cluster part, clusters try to remove noise from their own sub-patterns. As we will see shortly, each cluster succeeds in correcting a single error with high probability. Such individual error correction performance is fairly limited. The inter-cluster part capitalizes on the overlap among clusters to improve the overall performance of the recall phase. In what follows, we describe both parts in more details.

5.1 Intra-cluster Recall Algorithm

For the intra-cluster part, shown in Algorithm 2, we exploit the fact that the connectivity matrix of the neural network in each cluster is sparse and orthogonal to the memorized patterns. As a result we have $W^{(\ell)}(x^{(\ell)} + e^{(\ell)}) = W^{(\ell)}e^{(\ell)}$ where $e^{(\ell)}$ is the noise added to the sub-pattern $x^{(\ell)}$.

Algorithm 2 performs a series of *forward* and *backward* iterations to remove $e^{(\ell)}$. At each iteration, the pattern neurons decide locally whether to update their current state or not: if the amount of feedback received by a pattern neuron exceeds a threshold, the neuron updates its state, and remains intact, otherwise.³

In order to state our results, we need to define the *degree distribution polynomial* (from the node perspective). More precisely, let $\Lambda_i^{(\ell)}$ be the fraction of *pattern neurons* with degree i in cluster $G^{(\ell)}$ and define $\Lambda^{(\ell)}(x) = \sum_i \Lambda_i^{(\ell)} x^i$ to be the degree distribution polynomial for the pattern neurons in cluster ℓ . In principle $\Lambda^{(\ell)}(x)$ encapsulates all the information we need to know regarding cluster $G^{(\ell)}$, namely, the degree distribution. The following theorem provides a lower bound on the average probability of correcting a single erroneous pattern neuron by each cluster.

Theorem 3 *If we sample the neural graph randomly from $\Lambda^{(\ell)}(x)$, and let $\varphi \rightarrow 1$, then Algorithm 2 can correct (at least) a single error in cluster $G^{(\ell)}$ with probability at least*

$$P_c^{(\ell)} = \left(1 - \Lambda^{(\ell)}\left(\frac{\bar{d}_\ell}{m_\ell}\right)\right)^{n_\ell - 1},$$

where \bar{d}_ℓ , n_ℓ , and m_ℓ are the average degree of pattern neurons, the number of pattern neurons, and the number of constraint neurons in cluster $G^{(\ell)}$, respectively.

³In order to maintain the current value of a neuron, we can add self-loops to pattern neurons in Figure 1. the self-loops are not shown in the figure for the sake of clarity).

⁴In practice, we usually set $y_i^{(\ell)} = \text{sign}(h_i^{(\ell)})$ only if $|h_i^{(\ell)}| > \psi$, where ψ is a small positive threshold.

To gain some intuition we can further simplify the expression in the above theorem as follows

$$P_c^{(\ell)} \geq \left(1 - \left(\frac{\bar{d}_\ell}{m_\ell} \right)^{d_{\min}^{(\ell)}} \right)^{n_\ell - 1},$$

where $d_{\min}^{(\ell)}$ is the minimum degree of pattern neurons in cluster ℓ and we assumed that $d_{\min}^{(\ell)} \geq 1$. This shows the significance of having high-degree pattern neurons. In the extreme case of $d_{\min}^{(\ell)} = 0$ then we obtain the trivial bound of $P_c^{(\ell)} \geq (1 - \Lambda_0^{(\ell)})^{n_\ell - 1}$, where $\Lambda_0^{(\ell)}$ is the fraction of pattern neurons with degree equal to 0. In particular, for large n_ℓ we obtain $P_c^{(\ell)} \geq e^{-D_0^{(\ell)}}$, where $D_0^{(\ell)} = \Lambda_0^{(\ell)} n_\ell$ is the total number of pattern neurons with degree 0. Thus, even if only a single pattern neuron has a zero degree, probability of correcting a single error drops significantly.

While Theorem 3 provides a lower bound on the probability of correcting a single error when the connectivity graph is sampled according to the degree distribution polynomial $\Lambda^{(\ell)}(x)$, the following lemma shows that under mild conditions (that depends on the neighborhood relationship among neurons), Algorithm 2 will correct a single input error with probability 1.

Lemma 4 *If no two pattern neurons share the exact same neighborhood in cluster $G^{(\ell)}$, and as $\varphi \rightarrow 1$, Algorithm 2 corrects (at least) a single error.*

For the remaining of the paper we let $P_c = \mathbb{E}_\ell \left(P_c^{(\ell)} \right)$ denote this average probability of correcting one error averaged over all clusters. Lemma 4 suggests that under mild conditions, and in fact in many practical settings discussed later, P_c is close to 1. Thus, from now on we pessimistically assume that if there is a single error in a given cluster, Algorithm 2 corrects it with probability P_c and declares a failure if there are more than one error.

5.2 Inter-cluster Recall Algorithms

As mentioned earlier, the error correction ability of Algorithm 2 is fairly limited. As a result, if clusters work independently, they cannot correct more than a few external errors. However, as clusters overlap their combined performance can potentially be much better. Basically, they can help each other in resolving external errors: a cluster whose pattern neurons are in their correct states can provide truthful information to neighboring clusters. Figure 5 illustrates this idea.

This property is exploited in the inter-cluster recall approach, formally given by Algorithm 3. In words, the inter-cluster approach proceeds by applying Algorithm 2 in a round-robin fashion to each cluster. Clusters either eliminate their

internal noise in which case they keep their new states and can now help other clusters, or revert back to their original states. Note that by such a scheduling scheme, neurons can only change their states towards correct values.

The inter-cluster algorithm is in spirit similar to a famous decoding algorithm in communication systems for erasure channels, called the *peeling algorithm* (Luby et al., 2001). To make the connection more concrete, we first need to define a *contracted* version of the neural graph G as follows. In the contracted graph \tilde{G} , we compress all constraint nodes of a cluster $G^{(\ell)}$ into a single *super constraint node* $v^{(\ell)}$ (see Figure 6). Then, each super constraint node essentially acts as a check node capable of detecting and correcting any single error among its neighbors (i.e., pattern neurons). In contrast, it declares a failure if two or more of its neighbors are corrupted by noise. Once an error is corrected by a cluster, the number of errors in overlapping clusters may also reduce which in turn help them to eliminate their errors.

Through introducing the contracted graph, the similarity to the Peeling Decoder is now evident: in the Peeling Decoder, each constraint (so called checksum) node is capable of correcting a single erasure among its neighbors. Similarly, if there are more than one erasure among the neighbors, the checksum node declares erasure. However, once an erasure is eliminated by a checksum node, it helps other constraint nodes, namely those connected to the recently-eliminated erased node, as they will have one less erasure among their neighbors to deal with.

Based on the above similarity, we borrow methods from modern coding theory to obtain theoretical guarantees on the error rate of our proposed recall algorithm. More specifically, we use Density Evolution (DE), first developed by Luby et al. (2001) and generalized by Richardson and Urbanke (2008), to accurately bound the error correction performance.

Let $\tilde{\lambda}_i$ (resp. $\tilde{\rho}_j$) denote the fraction of *edges* that are adjacent to pattern (resp. constraint) nodes of degree i (resp. j). We call $\{\tilde{\lambda}_1, \dots, \tilde{\lambda}_L\}$ the pattern degree distribution and $\{\tilde{\rho}_1, \dots, \tilde{\rho}_n\}$ the super constraint degree distribution. Similar to Section 5.1, it is convenient to define the degree distribution polynomials as follows:

$$\begin{aligned}\tilde{\lambda}(z) &= \sum_i \tilde{\lambda}_i z^{i-1}, \\ \tilde{\rho}(z) &= \sum_i \rho_i z^{i-1}.\end{aligned}$$

Now consider a given cluster $v^{(\ell)}$ and a pattern neuron x connected to $v^{(\ell)}$. The *decision subgraph* of x is defined as the subgraph rooted at x and branched out from the super constraint nodes, excluding $v^{(\ell)}$. If the decision subgraph is a tree up to a depth of τ (meaning that no node appears more than once), we say that

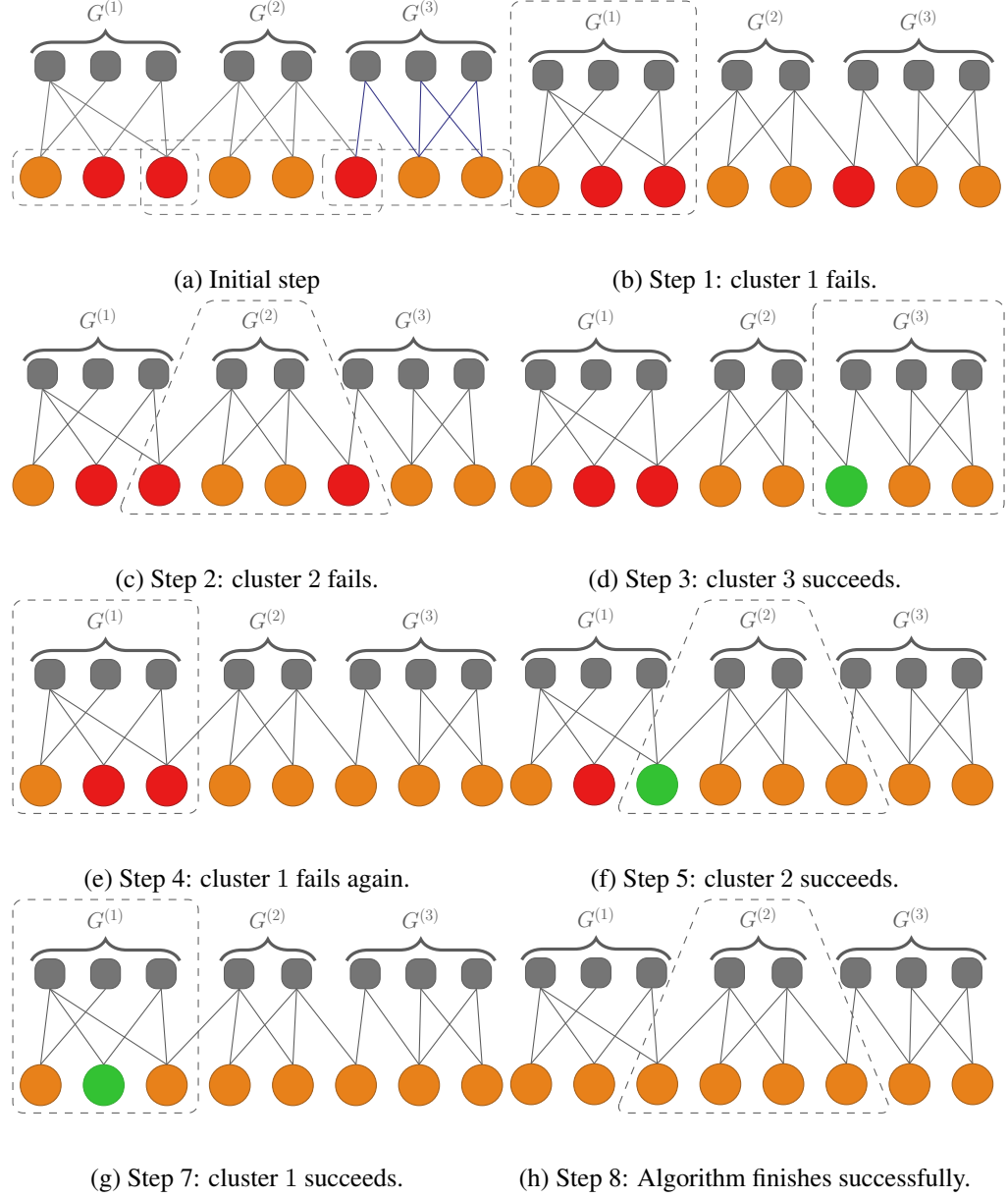


Figure 5: How overlaps among clusters help the neural network to achieve better error correction performance. We assume that each cluster can correct one input error. In other words, if the number of input errors are higher than one the cluster declares a failure.

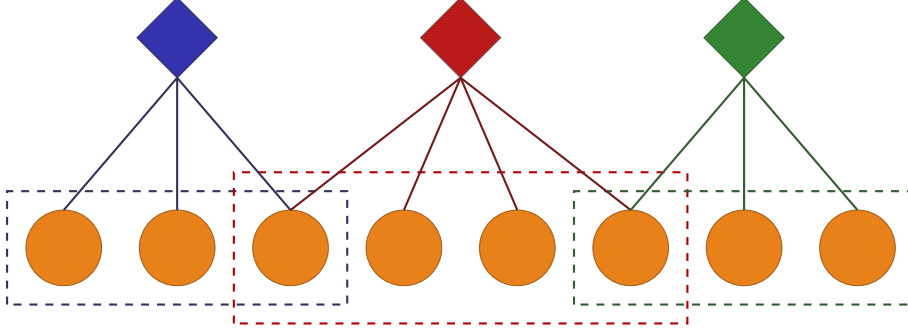


Figure 6: Contraction graph \tilde{G} corresponding to graph G in Figure 1.

the *tree assumption* holds for τ levels. An example of the decision subgraph is shown in Figure 7. Finally, we say that the node $v^{(\ell)}$ is unsatisfied if it is connected to a noisy pattern node. Recall that P_c denotes the average probability of a super constraint node correcting a single error among its neighbors.

Theorem 5 *Assume that \tilde{G} is chosen randomly according to the degree distribution pair $\tilde{\lambda}$ and $\tilde{\rho}$. Then, as the number of vertices of G grows large, Algorithm 3 will succeed in correcting all errors with high probability as long as $p_e \tilde{\lambda}(1 - P_c \tilde{\rho}(1 - z)) < z$ for $z \in (0, p_e)$.*

It is worth to make a few remarks about Theorem 5. First, the condition given in Theorem 5 can be used to calculate the maximal fraction of errors Algorithm 3 can correct. For instance, for the degree distribution pair $(\tilde{\lambda}(z) = z^2, \tilde{\rho}(z) = z^5)$, the threshold is $p_e^* \approx 0.429$, below which Algorithm 3 corrects all the errors with high probability. Second, the predicted threshold by Theorem 5 is based on the pessimistic assumption that a cluster can only correct a single error. Third, for a graph \tilde{G} , constructed randomly according to given degree distributions $\tilde{\lambda}$ and $\tilde{\rho}$, as the graph size grows the decision subgraph becomes a tree with probability close to 1. Hence, it can be shown (see, for example Richardson and Urbanke, 2008) that the recall performance for any such graphs will be *concentrated* around the average case given by Theorem 5.

6 Pattern Retrieval Capacity

Before discussing the the pattern retrieval capacity, we should note that the number of patterns C does not have any effect on the learning or recall algorithm except for its obvious influence on the learning time. More precisely, as long as the

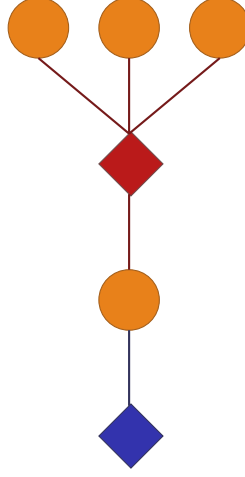


Figure 7: The decision subgraph of depth 2 for the third edge (from left) in Figure 6.

(sub)patterns lie on a subspace, the learning Algorithm 1 yields a matrix W that is orthogonal to all the patterns of the training set. Similarly, in the recall phase, algorithms 2 and 3 only need to compute $W \cdot e$ for the noise vector e .

Remember that the retrieval capacity is defined as the maximum number of patterns that a neural of size n is able to store. Hence, in order to show that the pattern retrieval capacity of our method is exponential in n , we need to demonstrate that there *exists* a training set \mathcal{X} with C patterns of length n for which $C \propto a^{rn}$, for some $a > 1$ and $0 < r < 1$.

Theorem 6 *Let \mathcal{X} be a $C \times n$ matrix formed by C vectors of length n with entries from \mathcal{Q} . Furthermore, let $k = \lfloor rn \rfloor$ for some $0 < r < 1$ and $k < \min_{\ell}(n_{\ell})$. Then, there exists a set of vectors of size $C = \Omega(a^{rn})$ with some $a > 1$ such that $\text{rank}(\mathcal{X}) = k < n$. Moreover, Algorithm 1 can learn this set.*

The proof is by construction. This construction can be used to synthetically generate patterns that lie in a subspace.

7 Experimental Results

In this section we evaluate the performance of our proposed algorithms over synthetic and natural datasets ⁵.

⁵The codes used in this paper are all available online at <http://goo.gl/ifR14t>.

7.1 Synthetic Scenario

A systematic way to generate patterns satisfying a set of linear constraints is outlined in the proof of Theorem 6. This proof is constructive and provides an easy way to randomly sample patterns with linear constraints. In our simulations, we consider a neural network in which each pattern neuron is connected to approximately 5 clusters. The number of connections should be neither too small (to ensure information propagation) nor too big (to adhere to the sparsity requirement).

In the learning phase, Algorithm 1 is performed (in parallel) for each cluster in order to find the connectivity matrix W . In the recall phase (and at each round), a pattern x is sampled uniformly at random from the training set. Then, each of its entries are corrupted with ± 1 additive noise independently with probability p_e . Algorithm 3 is subsequently used to denoise the corrupted patterns. We average out this process over many trials to calculate the error rate and compare it to the analytic bound derived in Theorem 5.

7.1.1 Learning Results

The left and right panels in Figure 8 illustrate the degree distributions of pattern and constraint neurons, respectively, over an ensemble of 5 randomly generated datasets. The network size is $n = 400$, which is divided into 50 overlapping clusters, each of size around 40, i.e., $n_\ell \simeq 40$ for $\ell = 1, \dots, 50$. Each pattern neuron is connected to 5 clusters, on average. The horizontal axis shows the normalized degree of pattern (resp., constraint) neurons and the vertical axis represents the fraction of neurons with the given normalized degree. The normalization is done with respect to the number of pattern (resp., constrain) neurons in the cluster. The parameters for the learning algorithm are $\alpha_t \propto 0.95/t$, $\eta = 0.75/\alpha_t$ and $\theta_t \propto 0.05/t$.

Figure 9 illustrates the same results for a network of size $n = 960$, which is divided into 60 clusters, each with size 80, on average. The learning parameters are the same as before, i.e., $\alpha_t \propto 0.95/t$, $\eta = 0.75/\alpha_t$ and $\theta_t \propto 0.05/t$, and each pattern neuron is connected to 5 clusters on average. Note that the overall normalized degrees are smaller compared to the case of $n = 400$, which indicates sparser clusters on average. In almost all cases that we have tried, the learning phase converges within two learning iterations, i.e., by going over the data set only twice.

7.1.2 Recall Results

Figure 10 illustrates the performance of the recall algorithm. The horizontal and vertical axes represent the average fraction of erroneous neurons and the final Pat-

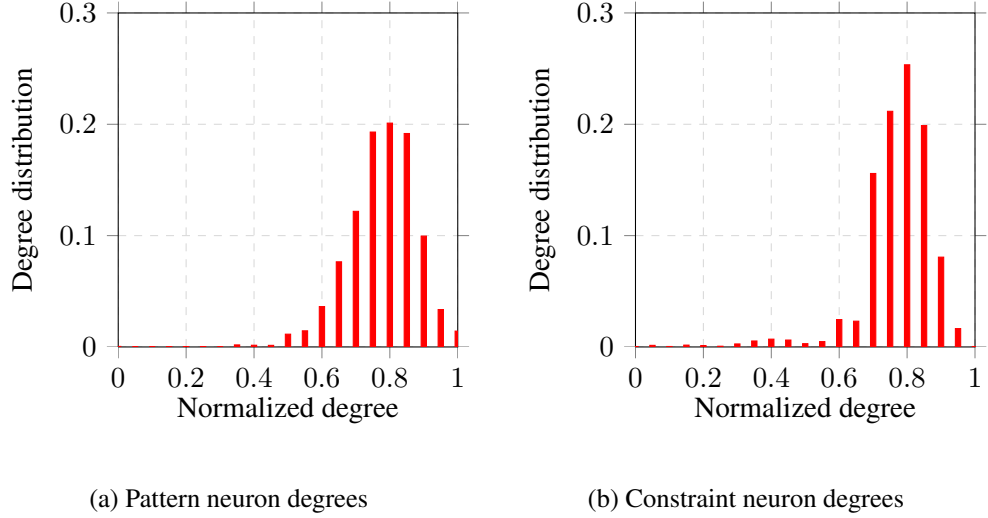


Figure 8: Pattern and constraint neuron degree distributions for $n = 400$, $L = 50$, and an average of 20 constraints per cluster. The learning parameters are $\alpha_t \propto 0.95/t$, $\eta = 0.75/\alpha_t$ and $\theta_t \propto 0.05/t$.

tern Error Rate (PER), respectively. The performance is compared against the theoretical bound derived in Theorem 5 as well as the two constructions proposed by Kumar et al. (2011) and Salavati and Karbasi (2012). The parameters used for this simulation are $n = 400$, $L = 50$ and $\varphi = 0.82$. For the *non-overlapping* clusters approach proposed by Salavati and Karbasi (2012), the network size is $n = 400$ with 4 clusters in the first level and one cluster in the second level (identical to their simulations). The convolutional neural network proposed in this paper clearly outperforms the prior art. Note that for the theoretical estimates used in Figure 10, we both calculated the probability of correcting a single error by each cluster P_c (via the lower bound in Theorem 3), and by fixing it to $P_c = 1$. The corresponding curves in Figure 10 show that the later estimate is tighter, i.e., when each cluster can correct a single error with probability close to 1.

Figure 11 shows the final PER for the network with $n = 960$ and $L = 60$ clusters. Comparing the PER with that of a network with $n = 400$ neurons and $L = 50$ clusters, we witness a degraded performance. At first glance this might seem surprising as we increased both the network size and the number of clusters. However, the key point in determining the performance of Algorithm 3 is not the number of clusters but rather the size of the clusters and the cluster nodes degree distribution $\tilde{\rho}(x)$. In the network with $n = 960$, we have around 80 pattern neurons per cluster, while in the network with $n = 400$ we have around $n = 40$ neurons

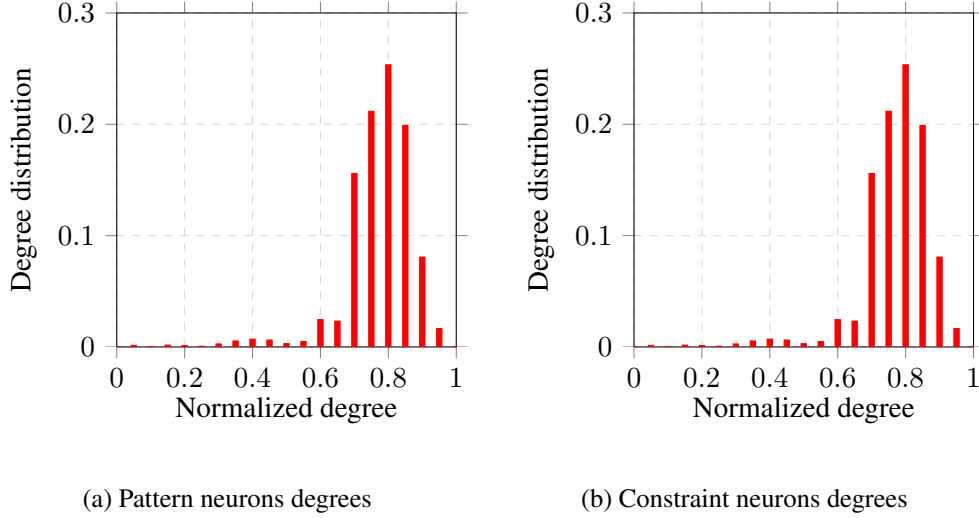


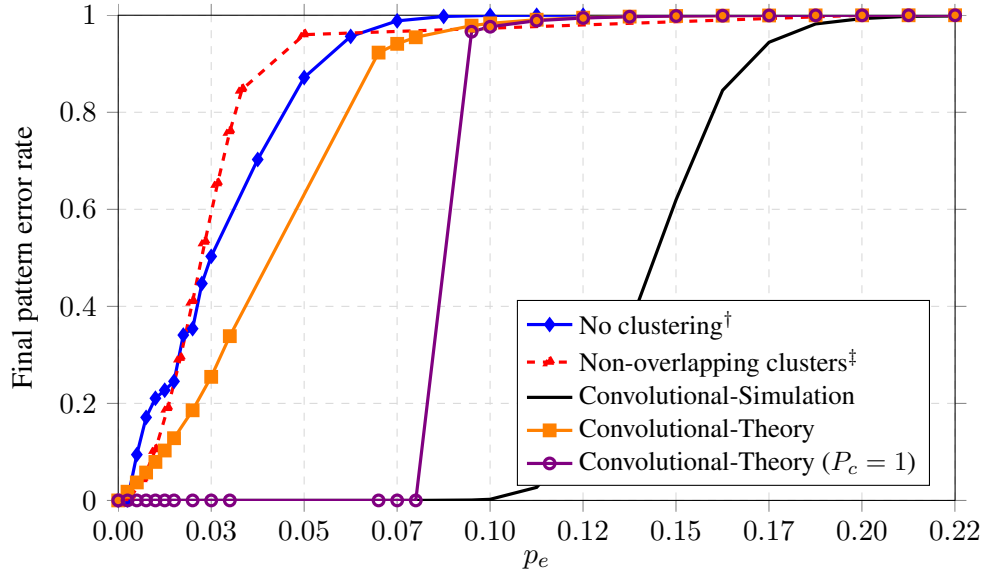
Figure 9: Pattern and constraint neuron degree distributions for $n = 960$, $L = 60$, and an average of 40 constraints per cluster. The learning parameters are $\alpha_t \propto 0.95/t$, $\eta = 0.75/\alpha_t$ and $\theta_t \propto 0.05/t$.

per cluster. Clearly, by increasing the network size without increasing the number of clusters, the chance of a cluster experiencing more than one error increases (remember, each cluster can correct a single error). This in turn results in an inferior performance. Hence, increasing the network size helps only if the number of clusters are increased correspondingly.

7.2 Real Datasets

So far, we have tested our proposed method over synthetic datasets where we generated patterns in such a way that they all belong to a subspace. In many real datasets (e.g., images and natural sounds), however, patterns rarely form a subspace. Rather, due to their common structures, they come very close to forming one. The focus of this section is to show how our proposed method can be adapted to such scenarios.

More specifically, let \mathcal{X} denote a dataset of C patterns of length n . Here we assume that patterns are all vectorized and form the rows of the matrix \mathcal{X} . The eigenvalues of the correlation matrix $A = \mathcal{X}^\top \mathcal{X}$ indicate how close the patterns are to a subspace. Note that A is a positive semidefinite matrix, so all eigenvalues are non-negative. In particular, if we have an eigenvalue 0 with positive multiplicity, then the patterns belong to a subspace. Similarly, if we have a set of eigenvalues



[†]: (Kumar et al., 2011), [‡]: (Salavati and Karbasi, 2012)

Figure 10: Recall error rate along with theoretical bounds for different architectures of network with $n = 400$ pattern neurons and $L = 50$ clusters. We compare the performance of our method with two other constructions where either no notion of cluster was considered (Kumar et al., 2011) or no overlaps between clusters was assumed (Salavati and Karbasi, 2012).

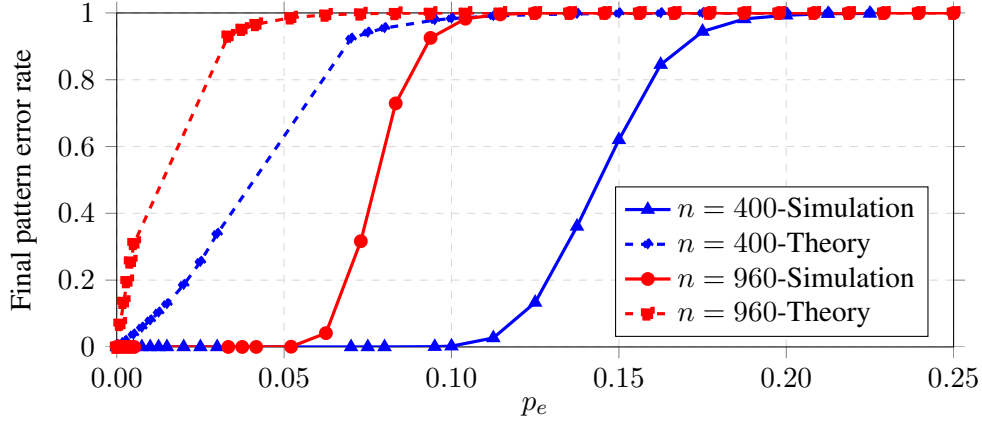


Figure 11: Recall error rate and the theoretical bounds for different architectures of network with $n = 960$ and $n = 400$ pattern neurons and $L = 60$ and $L = 50$ clusters, respectively..

all close to zero, then the patterns are close to a subspace of the n -dimensional space. Figure 12 illustrates the eigenvalue distribution of the correlation matrix for a dataset of $C = 10000$ gray-scale images of size 32×32 , sampled from 10 classes of the CIFAR-10 dataset (Krizhevsky and Hinton, 2009). Each image is quantized to 16 levels. Based on our notation, $n = 1024$ and $Q = 16$. As evident from the figure, almost half of the 1024 eigenvalues are less than 0.001, suggesting that the patterns are very close to a subspace.

7.2.1 Simulation Scenario

In order to adapt our method to this new scenario where patterns *approximately* belong to a subspace, we need to slightly modify the learning and the recall algorithms. We use CIFAR-10 dataset as the running example, however, the principles described below can be easily applied to other datasets.

To start, we first alter the way patterns are represented in such a way that is makes them easier to learn for our algorithm. More specifically, since the images are quantized to 16 levels, we can represent a 16-level pixel with 4 bits. As such, instead of having 1024 integer-valued pattern neurons to represent the patterns in the dataset, we will have 4096 binary pattern neurons. We adopt this modified description as it facilitates the learning process.

We then apply Algorithm 1 as before to learn the patterns in the dataset. Obviously, since the patterns do not exactly form a subspace, we cannot expect the

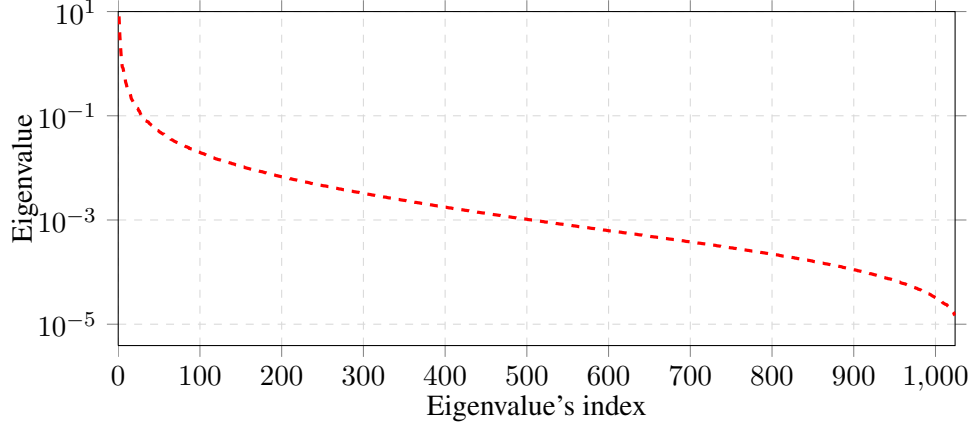


Figure 12: The eigenvalues of a dataset with 1000 gray-scale images of size 32×32 , uniformly sampled from 10 classes of the CIFAR-10 dataset (Krizhevsky and Hinton, 2009).

algorithm to finish with a weight vector w that is *orthogonal* to all the patterns. Nevertheless, by applying the learning algorithm, we will have a weight vector whose projection on the patterns is rather small. Following the same procedure as before, we obtain L neural graphs, $W^{(1)}, \dots, W^{(L)}$, for each of the L clusters. Note again that $W^{(i)}$'s are approximately (rather than exactly) orthogonal to the (sub-)patterns.

Our main observation is the following. We can interpret the deviation from the subspace as noise. Consequently, if we apply the intra-cluster recall method (Algorithm 2) to the patterns, we can find out what the network has actually learned in response to original patterns from the dataset \mathcal{X} . In other words, Algorithm 2 identifies the projection of original patterns to a subspace \mathcal{X}' . Hence, all the learned patterns are orthogonal to the connectivity matrix W . This idea is shown in figure 13, where we have the original image (left), the quantized version (middle), and the image learned by the proposed algorithm. It is worth observing that what the network has learned focuses more on the actual objects rather than unnecessary details.

For the recall phase, the approach is similar to before: we are given a set of noisy patterns and the goal is to retrieve the correct versions. In our simulations, we assume that the noise is added to the learned patterns (see above) but we can also consider the situation where noise is added to the quantized patterns.

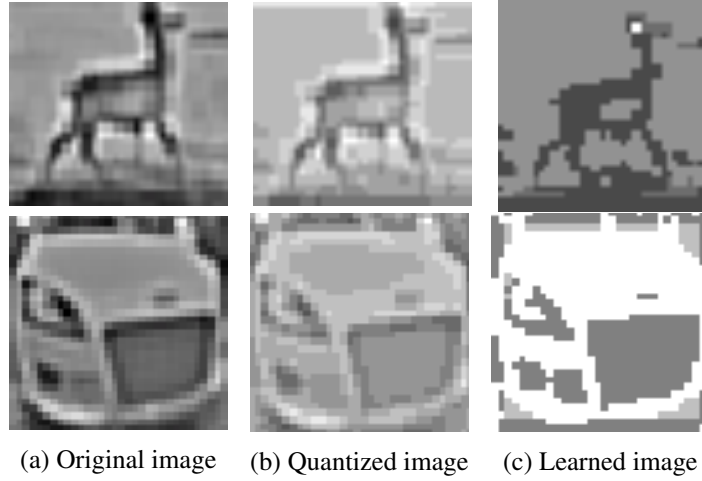


Figure 13: Original vs. learned images

7.2.2 Learning Results

Figure 14 illustrates the average cost (defined by $E(w^{(\ell)}(t))$ in Section 4.1) for learning one constraint vector versus the number of iterations. In this example, the learning parameters are $\alpha_0 = 0.95/t$, $\eta = 1$ and $\theta_t = 0.01/t$. The considered neural network has $n = 4096$ pattern neurons and $L = 401$ clusters of size 100. The learning process terminates if a) an orthogonal weight vector is found or b) 200 iterations is done.

Figure 15 illustrates the required number of iterations of Algorithm 1 so that a weight vector orthogonal to the patterns in the dataset \mathcal{X}' is obtained. As we see from the figure, in the majority of the cases, one pass over the dataset is enough. As before, we have $\alpha_0 = 0.95/t$, $\eta = 1$ and $\theta_t = 0.01/t$.

Furthermore, we have also uploaded a short video clip of the learning algorithm in action (i.e., iteration by iteration) for a few sample images from the dataset. The clip is available through the following link: <http://goo.gl/evcNOh>.

7.2.3 Recall Results

Figures 16 and 17 show the recall error rate as we increase the noise level for the neural network used in Sec 7.2.2. The update thresholds for the recall algorithm are set to $\varphi = 0.85$ and $\psi = 0.005$. The inter-module recall procedure (Algorithm 3) is performed at most 80 times and the corresponding error rates are calculated by evaluating the difference between the final state of pattern neurons (after running

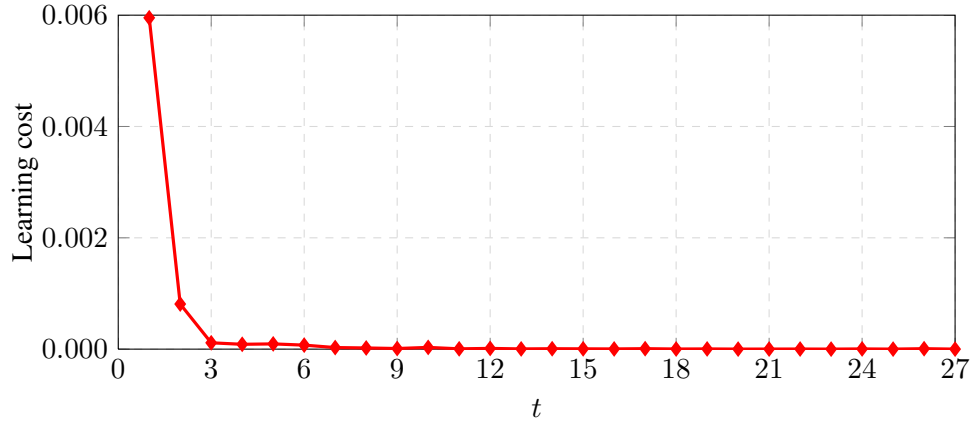


Figure 14: Average cost versus time for learning a weight vector in a network with $n = 4096$ pattern neurons and $L = 401$ clusters. The size of clusters is set to 100 with (around) 50 constraints in each cluster.

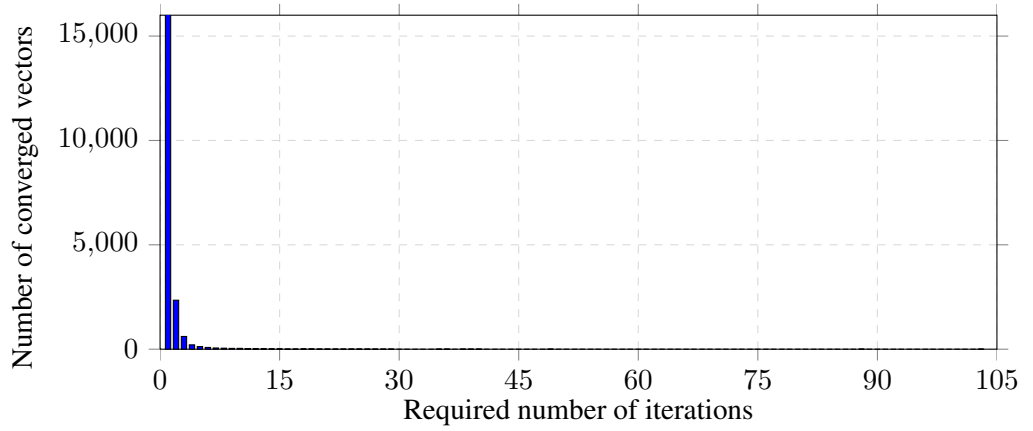


Figure 15: Number of the iterations required for Algorithm 1 to learn a vector orthogonal to the patterns in the dataset \mathcal{X}' , in a network with $n = 4096$ pattern neurons and $L = 401$ clusters of size 100 and (around) 50 constraints in each cluster.

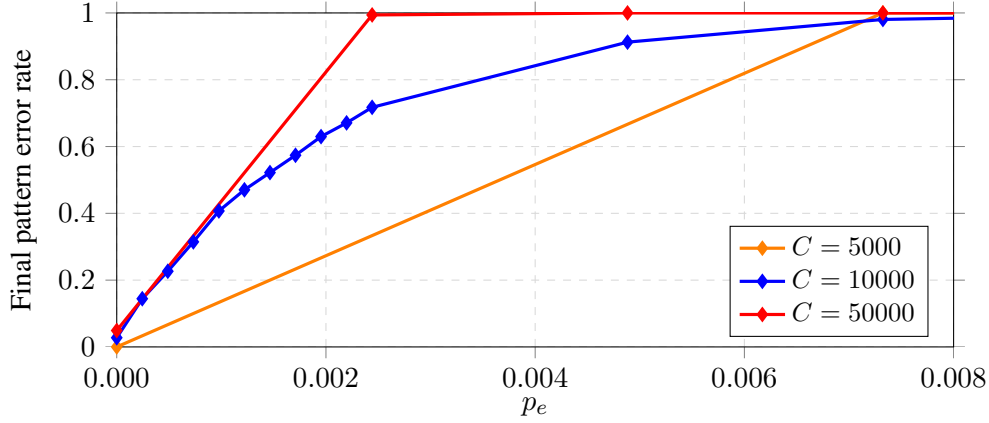


Figure 16: Recall error rate for a network with $n = 4096$ pattern neurons and $L = 401$ clusters, with cluster size equal to $n_\ell = 100$. The proposed recal method was applied to a dataset of 10000 images sampled from the CIFAR-10 database

Algorithm 3) and the noise-free patterns in the dataset \mathcal{X}' .

Figure 18 illustrates a few instances of the recalled images. In this figure, we have the original images (first column), the learned images (second column), the noisy versions (third column), and the recalled images (forth column). The figure also shows the input and the output Signal to Noise Ratios (SNR) for each example. Note that in all examples the SNR increases as we apply our recall algorithm. For this example we chose $\varphi = 0.95$ and $\psi = 0.025$. We have also uploaded a short video clip of the recall algorithm in action for a few sample images from the dataset, which can be found on <http://goo.gl/EHJfds>.

8 Analysis

This section contains the proofs of all theorems and technical lemmas we used in the paper.

8.1 Proof of Lemma 1

We proceed by induction. To this end, assume $\|w^{(\ell)}(t)\|_2 > 0$ and let

$$\dot{w}^{(\ell)}(t) = w^{(\ell)}(t) - \alpha_t y^{(\ell)}(t) \left(x^{(\ell)}(t) - \frac{y^{(\ell)}(t) w^{(\ell)}(t)}{\|w^{(\ell)}(t)\|_2^2} \right).$$

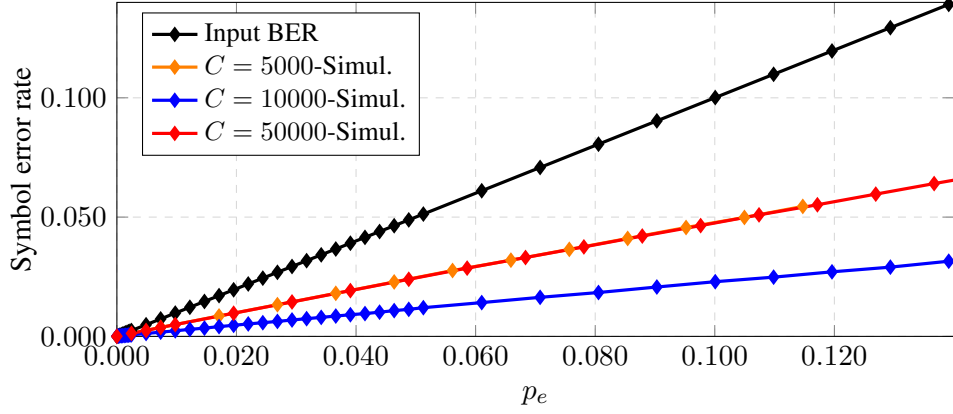


Figure 17: Symbol error rates for a network with $n = 4096$ pattern neurons and $L = 401$ clusters, applied to a dataset of 10000 images sampled from the CIFAR-10 database.

Note that

$$\|\dot{w}^{(\ell)}(t)\|_2^2 = \|w^{(\ell)}(t)\|_2^2 + \alpha_t^2 y^{(\ell)}(t)^2 \|x^{(\ell)}(t) - \frac{y^{(\ell)}(t)w^{(\ell)}(t)}{\|w^{(\ell)}(t)\|_2^2}\|_2^2 \geq \|w^{(\ell)}(t)\|_2^2 > 0.$$

Now,

$$\begin{aligned} \|w^{(\ell)}(t+1)\|_2^2 &= \|\dot{w}^{(\ell)}(t)\|_2^2 + \alpha_t^2 \eta^2 \|\Gamma(w^{(\ell)}(t), \theta_t)\|_2^2 - 2\alpha_t \eta \langle \Gamma(w^{(\ell)}(t), \theta_t), \dot{w}^{(\ell)}(t) \rangle \\ &\geq \|\dot{w}^{(\ell)}(t)\|_2^2 + \alpha_t^2 \eta^2 \|\Gamma(w^{(\ell)}(t), \theta_t)\|_2^2 - 2\alpha_t \eta \|\Gamma(w^{(\ell)}(t), \theta_t)\|_2 \|\dot{w}^{(\ell)}(t)\|_2 \\ &= \left(\|\dot{w}^{(\ell)}(t)\|_2 - \alpha_t \eta \|\Gamma(w^{(\ell)}(t), \theta_t)\|_2 \right)^2 \end{aligned}$$

Thus, in order to have $\|w^{(\ell)}(t+1)\|_2 > 0$, we must have that

$$\|\dot{w}^{(\ell)}(t)\|_2 - \alpha_t \eta \|\Gamma(w^{(\ell)}(t), \theta_t)\|_2 > 0.$$

Given that

$$\|\Gamma(w^{(\ell)}(t), \theta_t)\|_2 \leq \|w^{(\ell)}(t)\|_2 \leq \|\dot{w}^{(\ell)}(t)\|_2,$$

it is sufficient to have $\alpha_t \eta < 1$ in order to achieve the desired inequality. This proves the lemma.

8.2 Proof of Theorem 2

Let us define the *correlation* matrix for the sub-patterns that lie within the domain of cluster ℓ as follows

$$A^{(\ell)} := \mathbb{E}\{x^{(\ell)}(x^{(\ell)})^T | x \in \mathcal{X}\}.$$

Also, let us define

$$A_t^{(\ell)} := x^{(\ell)}(t)(x^{(\ell)}(t))^\top.$$

Hence, we have $A^{(\ell)} = \mathbb{E}(A_t^{(\ell)})$. Furthermore, recall the learning cost function

$$E(t) = E(w^{(\ell)}(t)) = \frac{1}{C} \sum_{\mu=1}^C \left(\langle w^{(\ell)}(t), x^\mu \rangle \right)^2.$$

From Alg. 1 we have

$$w^{(\ell)}(t+1) = w^{(\ell)}(t) - \alpha_t \left(y^{(\ell)}(t) \left(x^{(\ell)}(t) - \frac{y^{(\ell)}(t)w^{(\ell)}(t)}{\|w^{(\ell)}(t)\|_2^2} \right) + \eta \Gamma(w^{(\ell)}(t), \theta_t) \right).$$

Let

$$Y^{(\ell)}(t) = \mathbb{E}_x(\mathcal{X}^{(\ell)} w^{(\ell)}(t)),$$

where $\mathbb{E}_x(\cdot)$ is the expectation over the choice of pattern $x(t)$ and $\mathcal{X}^{(\ell)}$ is the matrix of all the sub-patterns corresponding to cluster ℓ in the dataset. Thus, we will have

$$Y^{(\ell)}(t+1) = Y^{(\ell)}(t) \left(1 + \alpha_t \frac{\left(w^{(\ell)}(t) \right)^\top A^{(\ell)} w^{(\ell)}(t)}{\|w^{(\ell)}(t)\|_2^2} \right) - \alpha_t \left(\mathcal{X}^{(\ell)} A^{(\ell)} w^{(\ell)}(t) + \eta \mathcal{X}^{(\ell)} \Gamma(w^{(\ell)}(t), \theta_t) \right).$$

Noting that $E(t) = \frac{1}{C} \|Y^{(\ell)}(t)\|_2^2$, we obtain

$$\begin{aligned} E(t+1) &= E(t) \left(1 + \alpha_t \frac{\left(w^{(\ell)}(t) \right)^\top A^{(\ell)} w^{(\ell)}(t)}{\|w^{(\ell)}(t)\|_2^2} \right)^2 \\ &\quad + \frac{\alpha_t^2}{C} \|\mathcal{X}^{(\ell)} A^{(\ell)} w^{(\ell)}(t) + \eta \mathcal{X}^{(\ell)} \Gamma(w^{(\ell)}(t), \theta_t)\|_2^2 \\ &\quad - 2\alpha_t \left(1 + \alpha_t \frac{\left(w^{(\ell)}(t) \right)^\top A^{(\ell)} w^{(\ell)}(t)}{\|w^{(\ell)}(t)\|_2^2} \right) \left(\left(w^{(\ell)}(t) \right)^\top \left(A^{(\ell)} \right)^2 w^{(\ell)}(t) \right) \\ &\quad - 2\alpha_t \left(1 + \alpha_t \frac{\left(w^{(\ell)}(t) \right)^\top A^{(\ell)} w^{(\ell)}(t)}{\|w^{(\ell)}(t)\|_2^2} \right) \left(\eta \left(w^{(\ell)}(t) \right)^\top A^{(\ell)} \Gamma(w^{(\ell)}(t), \theta_t) \right) \end{aligned}$$

By omitting all the second order terms $O(\alpha_t^2)$, we obtain

$$\begin{aligned}
E(t+1) &\simeq E(t) \left(1 + 2\alpha_t \frac{\left(w^{(\ell)}(t)\right)^\top A^{(\ell)} w^{(\ell)}(t)}{\|w^{(\ell)}(t)\|_2^2} \right) \\
&\quad - 2\alpha_t \left(\left(w^{(\ell)}(t)\right)^\top \left(A^{(\ell)}\right)^2 w^{(\ell)}(t) + \eta \left(w^{(\ell)}(t)\right)^\top A^{(\ell)} \Gamma(w^{(\ell)}(t), \theta_t) \right) \\
&= E(t) - 2\alpha_t \left(\left(w^{(\ell)}(t)\right)^\top \left(A^{(\ell)}\right)^2 w^{(\ell)}(t) - \frac{\left(w^{(\ell)}(t)\right)^\top A^{(\ell)} w^{(\ell)}(t)}{\|w^{(\ell)}(t)\|_2^2} E(t) \right) \\
&\quad - 2\alpha_t \eta \left(w^{(\ell)}(t)\right)^\top A^{(\ell)} \Gamma(w^{(\ell)}(t), \theta_t) \tag{7}
\end{aligned}$$

Note that

$$\begin{aligned}
\alpha_t \eta \left\| \left(w^{(\ell)}(t)\right)^\top A^{(\ell)} \Gamma(w^{(\ell)}(t), \theta_t) \right\|_2 &\leq \alpha_t \eta \|w^{(\ell)}(t)\|_2 \|A^{(\ell)}\|_2 \|\Gamma(w^{(\ell)}(t), \theta_t)\|_2 \\
&\leq \alpha_t \eta \|w^{(\ell)}(t)\|_2 \|A^{(\ell)}\|_2 (\sqrt{n} \theta_t).
\end{aligned}$$

Since we have $\theta_t = \Theta(\alpha_t)$ and that

$$\alpha_t \eta \left\| \left(w^{(\ell)}(t)\right)^\top A^{(\ell)} \Gamma(w^{(\ell)}(t), \theta_t) \right\|_2 = O(\alpha_t^2)$$

we can further simplify (7) as follows

$$E(t+1) \simeq E(t) - 2\alpha_t \left(\left(w^{(\ell)}(t)\right)^\top \left(A^{(\ell)}\right)^2 w^{(\ell)}(t) - \frac{\left(w^{(\ell)}(t)\right)^\top A^{(\ell)} w^{(\ell)}(t)}{\|w^{(\ell)}(t)\|_2^2} E(t) \right).$$

Thus, in order to show that the algorithm converges, we need to show that

$$\left(\left(w^{(\ell)}(t)\right)^\top \left(A^{(\ell)}\right)^2 w^{(\ell)}(t) - \frac{\left(w^{(\ell)}(t)\right)^\top A^{(\ell)} w^{(\ell)}(t)}{\|w^{(\ell)}(t)\|_2^2} E(t) \right) \geq 0$$

which in turn implies $E(t+1) \leq E(t)$. By noting that

$$E(t) = \left(w^{(\ell)}(t)\right)^\top A^{(\ell)} w^{(\ell)}(t),$$

we must show that

$$\left(w^{(\ell)}\right)^\top \left(A^{(\ell)}\right)^2 w^{(\ell)} \geq \left(\left(w^{(\ell)}\right)^\top A^{(\ell)} w^{(\ell)} \right)^2 / \|w^{(\ell)}\|_2^2.$$

The left hand side is $\|A^{(\ell)}w^{(\ell)}\|_2^2$. For the right hand side, we have

$$\frac{\| (w^{(\ell)})^\top A^{(\ell)} w^{(\ell)} \|_2^2}{\|w^{(\ell)}\|_2^2} \leq \frac{\|w^{(\ell)}\|_2^2 \|A^{(\ell)}w^{(\ell)}\|_2^2}{\|w^{(\ell)}\|_2^2} = \|A^{(\ell)}w^{(\ell)}\|_2^2.$$

The above inequality shows that $E(t+1) \leq E(t)$, which readily implies that for sufficiently large number of iterations, the algorithm converges to a local minimum $\hat{w}^{(\ell)}$ where $E(\hat{w}^{(\ell)}) = 0$. From Lemma 1 we know that $\|\hat{w}^{(\ell)}\|_2 > 0$. Thus, the only solution for $E(\hat{w}^{(\ell)}) = \|\mathcal{X}^{(\ell)}\hat{w}^{(\ell)}\|_2^2 = 0$ is for $\hat{w}^{(\ell)}$ to be orthogonal to the patterns in the data set.

8.3 Proof of Theorem 3

In the case of a single error, we can easily show that the noisy pattern neuron will always be updated towards the correct direction in Algorithm 2. For simplicity, let's assume the first pattern neuron of cluster ℓ is the noisy one. Furthermore, let $z^{(\ell)} = [1, 0, \dots, 0]$ be the noise vector. Denoting the i^{th} column of the weight matrix by $W_i^{(\ell)}$, we will have

$$y^{(\ell)} = \text{sign}(z_1 W_1^{(\ell)}) = z_1 \text{sign}(W_1^{(\ell)}).$$

Hence, in Algorithm 2 we obtain $g_1^{(\ell)} = 1 > \varphi$. This means that the noisy node gets updated towards the correct direction.

Therefore, the only source of error would be a correct pattern neuron getting updated mistakenly. Let P_i denote the probability that a correct pattern neuron $x_i^{(\ell)}$ gets updated. This happens if $|g_i^{(\ell)}| > \varphi$. For $\varphi \rightarrow 1$, this is equivalent to having

$$\langle W_i^{(\ell)}, \text{sign}(z_1 W_1^{(\ell)}) \rangle = \|W_i^{(\ell)}\|_0.$$

However, in cases where the neighborhood of $x_i^{(\ell)}$ is different from the neighborhood of x_1 among the constraint nodes we have

$$\langle W_i^{(\ell)}, \text{sign}(W_1^{(\ell)}) \rangle < \|W_i^{(\ell)}\|_0.$$

More specifically, let $\mathcal{N}(x_i^{(\ell)})$ indicate the set of neighbors of $x_i^{(\ell)}$ among constraint neurons in cluster ℓ . Then in the case where

$$\mathcal{N}(x_i^{(\ell)}) \cap \mathcal{N}(x_1^{(\ell)}) \neq \mathcal{N}(x_i^{(\ell)}),$$

there are non-zero entries in $W_i^{(\ell)}$ while $W_1^{(\ell)}$ is zero, and vice-versa. Therefore, by letting P'_i to be the probability of $\mathcal{N}(x_i^{(\ell)}) \cap \mathcal{N}(x_1^{(\ell)}) = \mathcal{N}(x_i^{(\ell)})$, we note that

$$P_i \leq P'_i.$$

The above inequality help us obtain an upper bound on P_i , by bound P'_i . Since there is only one noisy neuron x_1 , we know that, on average, this node is connected to \bar{d}_ℓ constraint neurons which implies that the probability of x_i and x_1 sharing exactly the same neighborhood is:

$$P'_i = \left(\frac{\bar{d}_\ell}{m_\ell} \right)^{d_i},$$

where d_i is the degree of neuron x_i . By taking the average over the pattern neurons, we obtain the following bound on the average probability of a correct pattern neuron being mistakenly updated:

$$P'_e = \sum_{d_i} \Lambda_{d_i}^{(\ell)} P'_i = \sum_{d_i} \Lambda_{d_i}^{(\ell)} \left(\frac{\bar{d}_\ell}{m_\ell} \right)^{d_i} = \Lambda^{(\ell)} \left(\frac{\bar{d}_\ell}{m_\ell} \right),$$

where $\Lambda^{(\ell)}(x) = \sum_i \Lambda_i^{(\ell)} x^i$ is the degree distribution polynomial. Therefore, the probability of correcting one noisy input is lower bounded by $P_c^{(\ell)} \geq (1 - P'_e)^{n_\ell - 1}$, i.e.,

$$P_c^{(\ell)} \geq \left(1 - \Lambda^{(\ell)} \left(\frac{\bar{d}_\ell}{m_\ell} \right) \right)^{n_\ell - 1}.$$

This proves the theorem.

8.4 Proof of Lemma 4

Without loss of generality, suppose the first pattern neuron is contaminated by an external error +1, i.e., $z^{(\ell)} = [1, 0, \dots, 0]$. As a result

$$y^{(\ell)} = \text{sign} \left(W^{(\ell)}(x^{(\ell)} + z^{(\ell)}) \right) = \text{sign} \left(Wx^{(\ell)} + Wz^{(\ell)} \right) = \text{sign} \left(W^{(\ell)} z^{(\ell)} \right) = \text{sign} \left(W_1^{(\ell)} \right),$$

where $W_i^{(\ell)}$ is the i^{th} column of $W^{(\ell)}$. Hence, the feedback transmitted by the constraint neurons is $\text{sign}(W_1^{(\ell)})$. As a result, decision parameters of pattern neuron i , i.e., $g_i^{(\ell)}$ in Algorithm 2, will be

$$g_i^{(\ell)} = \frac{\langle \text{sign}(W_1^{(\ell)}), W_i^{(\ell)} \rangle}{\langle \text{sign}(W_i^{(\ell)}), W_i^{(\ell)} \rangle}.$$

Note that the denominator is simply $\|W_i^{(\ell)}\|_0 = \langle \text{sign}(W_i^{(\ell)}), W_i^{(\ell)} \rangle$. By assumption, no two pattern neurons in $G^{(\ell)}$ share the exact same set of neighbors. Therefore, for all $i, j \in \{1, \dots, n_\ell\}$ such that $i \neq j$, there is at least a non-zero entry, say k , in $W_j^{(\ell)}$ for which $W_{ik}^{(\ell)} = 0$. Thus, we have $g_i^{(\ell)} = 1$ if $i = 1$ and $g_i^{(\ell)} < 1$ if $i > 1$. As a result, for $\varphi \rightarrow 1$, only the first neuron (i.e., the noisy one) will update its value towards the correct state.

8.5 Proof of Theorem 5

The proof is, in spirit, similar to Theorem 3.50 of (Richardson and Urbanke, 2008). Consider a message transmitted over an edge from a given cluster node $v^{(\ell)}$ to a given *noisy* pattern neuron at iteration t of Algorithm 3. This message will be a failure, indicating that the super constraint node being unable to correct the error, if

1. the super constraint node $v^{(\ell)}$ receives at least one error message from its *other* neighbors among pattern neurons. This event happens if it is connected to more than one noisy pattern neuron.
2. the super constraint node $v^{(\ell)}$ does not receive an error message from any of its other neighbors but is unable to correct the single error in the given noisy neuron. This event happens with probability $1 - P_c$.

Let us denote the probability of the above failure message by $\pi^{(\ell)}(t)$ and the average probability that a pattern neuron sends an erroneous message to a neighboring cluster node by $z(t)$. Then, we have

$$\pi^{(\ell)}(t) = 1 - P_c(1 - z(t))^{\tilde{d}_\ell - 1},$$

where \tilde{d}_ℓ is the degree of the super constraint neuron $v^{(\ell)}$ in the contracted graph \tilde{G} . Similarly, let $\pi(t)$ denote the average probability that a super constraint node sends a message declaring the violation of at least one of its constraint neurons. Then we have

$$\pi(t) = \mathbb{E}_{\tilde{d}_\ell}(\pi^{(\ell)}(t)) = \sum_i \tilde{\rho}_i (1 - P_c(1 - z(t))^{\tilde{d}_i - 1}) = 1 - P_c \tilde{\rho}(1 - z(t)).$$

Now consider the message transmitted from a given pattern neuron x_i with degree d_i to a given super constraint node $v^{(\ell)}$ in iteration $t + 1$ of Algorithm 3. This message will indicate a noisy pattern neuron if the pattern neuron was noisy in the first place (with probability p_e) and all of its *other* neighbors among super constraint nodes has sent a violation message in iteration t . Therefore, the probability of this node being noisy will be $z(0)\pi(t)^{d_i - 1}$ where $z(0) = p_e$. Hence, the average probability that a pattern neuron remains noisy at $(t + 1)$ -th iteration is

$$z(t + 1) = p_e \sum_i \tilde{\lambda}_i \pi(t)^{i - 1} = p_e \cdot \tilde{\lambda}(\pi(t)) = p_e \cdot \tilde{\lambda}(1 - P_c \tilde{\rho}(1 - z(t))).$$

Note that the denoising operation will be successful if $z(t + 1) < z(t)$, $\forall t$. Therefore, we must look for the maximum p_e such that $p_e \tilde{\lambda}(1 - P_c \tilde{\rho}(1 - z)) < z$ for $z \in [0, p_e]$.

8.6 Proof of Theorem 6

The proof is based on construction: we build a data set \mathcal{X} with the required properties such that it can be memorized by the proposed neural network.

Consider a matrix $G \in \mathbb{R}^{k \times n}$ with rank $k = rn$ where $0 < r < 1$ is chosen such that $k < \min_{\ell}(n_{\ell})$. Let the entries of G be non-negative integers between 0 and $\gamma - 1$. Here we assume that $\gamma \geq 2$.

We start constructing the patterns in the data set as follows. We pick a random vector $u \in \mathbb{R}^k$ with integer-valued-entries between 0 and $v - 1$ where $v \geq 2$. We set the pattern $x \in \mathcal{X}$ to be $x = G^{\top}u$ if all the entries of x are between 0 and $Q - 1$. Since both u and G have only non-negative entries, all entries in x are non-negative. However, we need to design G such that all entries of $G^{\top}u$ be less than Q . Let g_j be the j -th column of G . Then, the j -th entry of x is equal to $x_j = \langle u, g_j \rangle$. Therefore,

$$x_j = u^{\top} g_j \leq d_j(\gamma - 1)(v - 1)$$

Let $d^* = \min_j d_j$. We can choose γ , v and d^* such that

$$Q - 1 \geq d^*(\gamma - 1)(v - 1)$$

which in turn ensures that all entries of x are less than Q . Furthermore, we have selected k in such a way that $k < \min_{\ell}(n_{\ell})$. As a result we are sure that the set of sub-patterns of the dataset \mathcal{X} form a subspace with dimension k in an n_{ℓ} -dimensional space. Since there are v^k vectors u with integer entries between 0 and $v - 1$, we have $v^k = v^{rn}$ patterns forming \mathcal{X} . This implies that the storage capacity $C = v^{rn}$ is an exponential number in n as long as $v \geq 2$.

9 Conclusions and Final Remarks

In this paper, we proposed the first neural network structure that learns an exponential number of patterns (in the size of the network) and corrects up to a linear fraction of errors. The main observation we made was that natural patterns seem to have inherent redundancy and we proposed a framework to capture redundancies that appear in the form of linear (or close to linear) constraints. Our experimental results also reveal that our learning algorithm can be seen as a feature extraction method, tailored for patterns with such constraints. Extending this line of thought through more sophisticated feature extraction approaches, and in light of recent developments in deep belief networks (Jarrett et al., 2009; Coates and Ng, 2011; Le et al., 2010; Vincent et al., 2008; Ngiam et al., 2011), is an interesting future direction to pursue.

References

- Emmanuel J. Candès and Terence Tao. Near-optimal signal recovery from random projections: Universal encoding strategies? *IEEE Transactions on Information Theory*, 52(12):5406–5425, 2006.
- Adam Coates and Andrew Ng. The importance of encoding versus training with sparse coding and vector quantization. In Lise Getoor and Tobias Scheffer, editors, *International Conference on Machine Learning (ICML)*, pages 921–928, New York, NY, USA, 2011. ACM.
- D. L. Donoho. Compressed sensing. *IEEE Transactions on Information Theory*, 52(4):1289–1306, 2006.
- David L. Donoho, A. Maleki, and A. Montanari. Message-passing algorithms for compressed sensing. *Proceedings of the National Academy of Sciences (PNAS)*, 106(45):18914–18919, 2009.
- Vincent Gripon and Claude Berrou. Sparse neural networks with large learning diversity. *IEEE Transactions on Neural Networks*, 22(7):1087–1096, 2011.
- Donald O. Hebb. *The Organization of Behavior: A Neuropsychological Theory*. Wiley & Sons, New York, 1949.
- John J. Hopfield. Neural networks and physical systems with emergent collective computational abilities. *Proc. Natl. Acad. Sci. U.S.A.*, 79(8):2554–2558, 1982.
- Stanislaw Jankowski, Andrzej Lozowski, and Jacek M. Zurada. Complex-valued multi-state neural associative memory. *IEEE Transactions on Neural Networks and Learning Systems*, 7(6):1491–1496, 1996.
- Kevin Jarrett, Koray Kavukcuoglu, Marc’Aurelio Ranzato, and Yann LeCun. What is the best multi-stage architecture for object recognition? In *IEEE International Conference on Computer Vision (ICCV)*, pages 2146–2153, 2009.
- Amin Karbasi, Amir Hesam Salavati, and Amin Shokrollahi. Iterative learning and denoising in convolutional neural associative memories. In *International Conference on Machine Learning (ICML)*, pages 445–453, 2013.
- Alex Krizhevsky and Geoffrey Hinton. Learning multiple layers of features from tiny images. *Master’s thesis, Department of Computer Science, University of Toronto*, 2009.
- K. Raj Kumar, Amir Hesam Salavati, and Mohammad A. Shokrollah. Exponential pattern retrieval capacity with non-binary associative memory. In *IEEE Information Theory Workshop (ITW)*, pages 80–84, 2011.
- K. Raj Kumar, Amir Hesam Salavati, and Mohammad A. Shokrollahi. A non-binary associative memory with exponential pattern retrieval capacity and iterative learning. *IEEE Transaction on Neural Networks and Learning systems*, 2014. To appear in.

- Quoc V. Le, Jiquan Ngiam, Zhenghao Chen, Daniel Jin hao Chia, Pang Wei Koh, and Andrew Y. Ng. Tiled convolutional neural networks. In *Advances in Neural Information Processing Systems (NIPS)*, pages 1279–1287, 2010.
- Donq-Liang Lee. Improvements of complex-valued Hopfield associative memory by using generalized projection rules. *IEEE Transactions on Neural Networks*, 17(5):1341–1347, 2006.
- Michael Luby, Michael Mitzenmacher, Mohammad Amin Shokrollahi, and Daniel A. Spielman. Efficient erasure correcting codes. *IEEE Transactions on Information Theory*, 47(2):569–584, 2001.
- Robert J. McEliece, Edward C. Posner, Eugene R. Rodemich, and Santosh S. Venkatesh. The capacity of the hopfield associative memory. *IEEE Transactions on Information Theory*, 33(4):461–482, 1987.
- Mehmet Kerem Muezzinoglu, Cuneyt Guzelis, and Jacek M. Zurada. A new design method for the complex-valued multistate hopfield associative memory. *IEEE Transactions on Neural Networks*, 14(4):891–899, 2003.
- Jiquan Ngiam, Pang Wei Koh, Zhenghao Chen, Sonia A. Bhaskar, and Andrew Y. Ng. Sparse filtering. In John Shawe-Taylor, Richard S. Zemel, Peter L. Bartlett, Fernando C. N. Pereira, and Kilian Q. Weinberger, editors, *Advances in Neural Information Processing Systems (NIPS)*, pages 1125–1133, 2011.
- Erkki Oja and Juha Karhunen. On stochastic approximation of the eigenvectors and eigenvalues of the expectation of a random matrix. *Math. Analysis and Applications*, 106: 69–84, 1985.
- Erkki Oja and Teuvo Kohonen. The subspace learning algorithm as a formalism for pattern recognition and neural networks. In *IEEE International Conference on Neural Networks*, volume 1, pages 277–284, 1988.
- P. Peretto and J. J. Niez. Long term memory storage capacity of multiconnected neural networks. *Biological Cybernetics*, 54(1):53–64, 1986.
- Tom Richardson and Ruediger Urbanke. *Modern Coding Theory*. Cambridge University Press, New York, NY, USA, 2008.
- Amir Hesam Salavati. *Coding theory and neural associative memories with exponential pattern retrieval capacity*. PhD thesis, Ecole Polytechnique federale de Lausanne (EPFL), 2014. URL http://algo.epfl.ch/~amir/PhD_Thesis_Salavati.pdf.
- Amir Hesam Salavati and Amin Karbasi. Multi-level error-resilient neural networks. In *IEEE International Symposium on Information Theory (ISIT)*, pages 1064–1068, 2012.

- Richard Socher, Jeffrey Pennington, Eric H Huang, Andrew Y Ng, and Christopher D Manning. Semi-supervised recursive autoencoders for predicting sentiment distributions. In *Proceedings of the Conference on Empirical Methods in Natural Language Processing*, pages 151–161. Association for Computational Linguistics, 2011.
- R. Tanner. A recursive approach to low complexity codes. *IEEE Transactions on Information Theory*, 27(5):533–547, 1981.
- Joel A. Tropp and Stephen J. Wright. Computational methods for sparse solution of linear inverse problems. *Proceedings of the IEEE*, 98(6):948–958, 2010.
- Santosh S Venkatesh. Connectivity versus capacity in the hebb rule. In *Theoretical Advances in Neural Computation and Learning*, pages 173–240. Springer, 1994.
- Santosh S. Venkatesh and Demetri Psaltis. Linear and logarithmic capacities in associative neural networks. *IEEE Transactions on Information Theory*, 35(3):558–568, 1989.
- Pascal Vincent, Hugo Larochelle, Yoshua Bengio, and Pierre-Antoine Manzagol. Extracting and composing robust features with denoising autoencoders. In *International Conference on Machine Learning (ICML)*, pages 1096–1103, New York, NY, USA, 2008. ACM.
- Lei Xu, Adam Krzyzak, and Erkki Oja. Neural nets for dual subspace pattern recognition method. *International Journal of Neural Systems*, 2(3):169–184, 1991.

Algorithm 1 Iterative Learning

Input: Dataset \mathcal{X} with $|\mathcal{X}| = C$, stopping point ε .

Output: $w^{(\ell)}$

- 1: **while** $\frac{1}{C} \sum_{x \in \mathcal{X}} |\langle x^{(\ell)}(t), w^{(\ell)}(t) \rangle|^2 > \varepsilon$ **do**
- 2: Choose pattern $x(t)$ uniformly at from \mathcal{X} .
- 3: Compute $y^{(\ell)}(t) = \langle x^{(\ell)}(t), w^{(\ell)}(t) \rangle$.
- 4: Update $w^{(\ell)}(t)$ as follows

$$w^{(\ell)}(t) = w^{(\ell)}(t-1) - \alpha_t \left(y^{(\ell)}(t) \left(x^{(\ell)}(t) - \frac{y^{(\ell)}(t) w^{(\ell)}(t-1)}{\|w^{(\ell)}(t-1)\|_2^2} \right) + \eta \Gamma(w^{(\ell)}(t-1), \theta_t) \right)$$

- 5: $t \leftarrow t + 1$.
 - 6: **end while**
-

Algorithm 2 Intra-cluster Error Correction

Input: Training set \mathcal{X} , threshold φ , iteration t_{\max}

Output: $x_1^{(\ell)}, x_2^{(\ell)}, \dots, x_{n_\ell}^{(\ell)}$

- 1: **for** $t = 1 \rightarrow t_{\max}$ **do**
- 2: *Forward iteration:* Calculate the weighted input sum $h_i^{(\ell)} = \sum_{j=1}^{n_\ell} W_{ij}^{(\ell)} x_j^{(\ell)}$, for each neuron $y_i^{(\ell)}$ and set $y_i^{(\ell)} = \text{sign}(h_i^{(\ell)})$.⁴
- 3: *Backward iteration:* Each neuron $x_j^{(\ell)}$ computes

$$g_j^{(\ell)} = \frac{\sum_{i=1}^{m_\ell} W_{ij}^{(\ell)} y_i^{(\ell)}}{\sum_{i=1}^{m_\ell} |W_{ij}^{(\ell)}|}.$$

- 4: Update the state of each pattern neuron j according to

$$x_j^{(\ell)} = x_j^{(\ell)} - \text{sign}(g_j^{(\ell)})$$

- 5: only if $|g_j^{(\ell)}| > \varphi$.
 - 5: $t \leftarrow t + 1$
 - 6: **end for**
-

Algorithm 3 Sequential Peeling Algorithm

Input: $\tilde{G}, G^{(1)}, G^{(2)}, \dots, G^{(L)}$.

Output: x_1, x_2, \dots, x_n

- 1: **while** There is an unsatisfied $v^{(\ell)}$, for $\ell = 1, \dots, L$ **do**
 - 2: **for** $\ell = 1 \rightarrow L$ **do**
 - 3: If $v^{(\ell)}$ is unsatisfied, apply Algorithm 2 to cluster $G^{(l)}$.
 - 4: If $v^{(\ell)}$ remained unsatisfied, revert the state of pattern neurons connected to $v^{(\ell)}$ to their initial state. Otherwise, keep their current states.
 - 5: **end for**
 - 6: **end while**
 - 7: Declare x_1, x_2, \dots, x_n if all $v^{(\ell)}$'s are satisfied. Otherwise, declare failure.
-

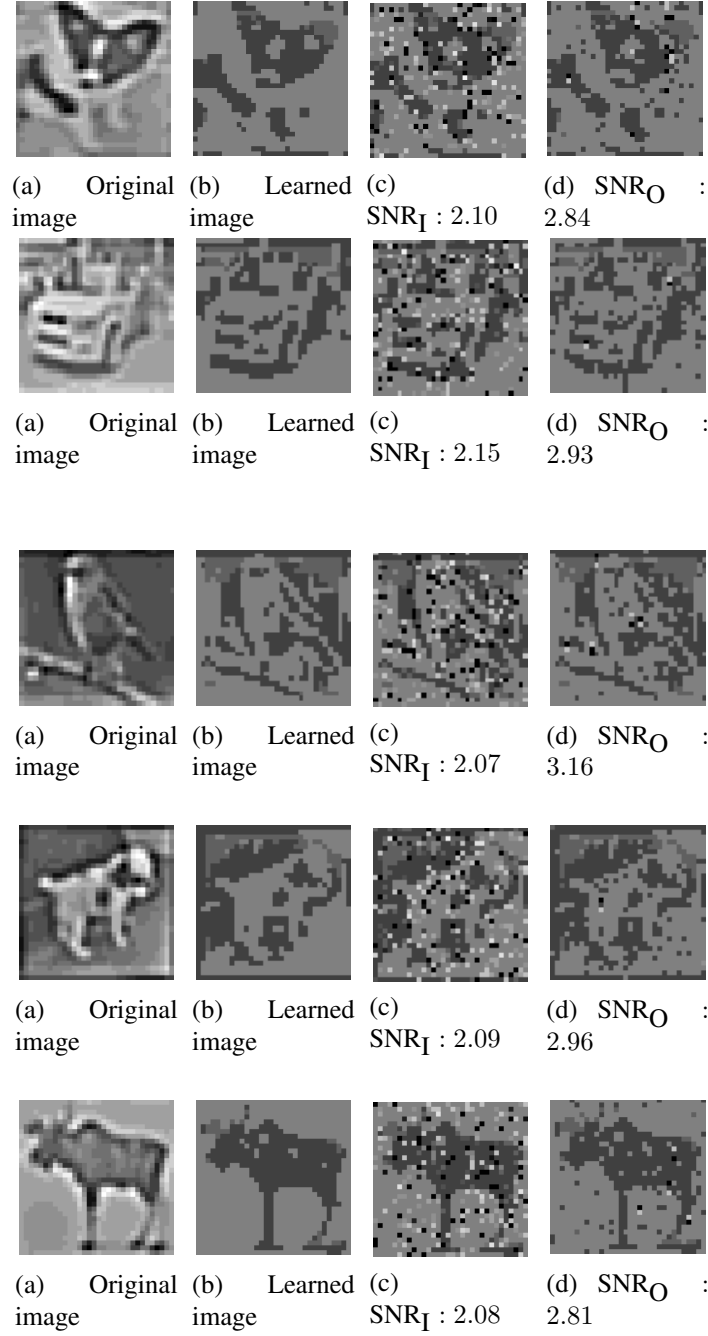


Figure 18: Examples of the learning and recall phase for images sampled from CIFAR-10. Here, SNR_I and SNR_O denote the input and output SNR's, respectively.